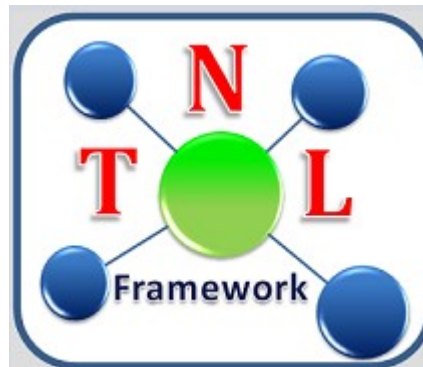


TNL

THz Spectroscopy Simulator User Manual

Material Characterization simulation Software



Tech Next Lab (P) Ltd

Building No. #417/22/A, Niwaz Ganj,
Near Napier Road Park, Lucknow - 226 003, (U.P.), India,
Tel: (+91) 522 404 1565,
Web: www.technextlab.com

21st March, 2022

Notice

The information contained in this document is subject to change without notice.

Tech Next Lab (P) Ltd is not liable for any kind of warranty related to this material. The limited warranty extends ONLY for warranty of fitness for a purpose of particular requirement.

Tech Next Lab (P) Ltd shall not be held liable for typographical errors contained in the material. The users of this manual will be solely responsible for use of this manual, for incidental or consequential damages in connection with the furnishing, and performance.

The FB (Full Band) Simulator manual contains proprietary information under the copyright laws. All copyrights are reserved to Tech Next Lab (P) Ltd. Without prior written consent, the photocopy, reproduction, or translation into other language of this manual is prohibited under copyright laws.

TNL Framework, TNL-EpiGrow simulator, TNL-FBS (Full Band) simulator, TNL-EMS (Electron Mobility) simulator, TNL-TSS (THz Spectroscopy) simulator, TNL-PDS (Particle Device) simulator, TNL-TSS (THz Spectroscopy) and TNL-Plot, StrViewer (TNL-Viewer) are the trademarks of **Tech Next Lab (P) Ltd.**

Copyright © 2015 - 2022, **Tech Next Lab (P) Ltd.**

Additional information is provided at:

<http://www.technextlab.com>

TNL

Contents

1. Introduction	5
1.1 TNL-TS simulator Overview	6
1.2 Need of TNL-TS simulator	6
1.3 Features	9
1.4 Benefits	10
2. Start using TNL-TS simulator	11
2.1 Getting Started	13
2.2 TNL-TS SIMULATOR window frame	14
2.2.1 Material Tab	15
2.2.2 Mechanism Tab	19
2.2.3 Output Tab	23
2.2.4 Other Button	24
2.3 Hands on Tutorial	25
3. Physics	30
3.1 Introduction	32
3.2 Hot Carrier Transportation	34
3.3 Scattering Mechanisms	37
3.3.1 Fermi's Golden Rule	39
3.3.2 Acoustic Deformation Potential Scattering	43
3.3.3 Non-Polar Optical Scattering	45
3.3.4 Polar Optical Phonon Scattering	46
3.3.5 Ionized Impurity Scattering	47
3.3.6 Alloy Scattering	48
3.3.7 Piezoelectric Scattering	49
3.3.8 Dislocation Scattering	50
3.3.9 Carrier-Carrier Scattering	51
3.3.10 Impact Ionization Scattering	52
3.4 Material Data Base	53
3.5 Free Flight Generation	56
3.6 Choice of Scattering Angles	59
3.7 Ensemble Monte Carlo Simulation	60
References	63

Blank Page

TNL

CHAPTER 1

INTRODUCTION



TNL

2.3 TNL-TS simulator Overview

TNL-TS simulator is a powerful tool to simulate hot carrier dynamics on three valleys over full electronic band structure due to interaction of THz pulse energy with carriers. The microscopic ultrafast carrier dynamics simulation considers the transportation of the individual particles in the presence of the forces acting on them due to external THz field as well as due to the internal fields of the crystal lattice and other charges in the system. In solids, such as semiconductors and metals, transport is known to be mainly dominated by random intrinsic and extrinsic scattering mechanisms e.g. carrier-carrier, defects, impurities, lattice vibrations, etc., and it randomize the momentum and energy of charge particles in time domain. Hence, stochastic techniques to model these random scattering events are particularly useful in describing electronic motion in semiconductors. The carrier motion is characterized by using Monte Carlo (MC) method for the solution of Boltzmann transport equation (BTE), which is coupled with non-linear scattering mechanisms with the flexibilities to users to input the number of carrier density over three valleys to analyze the transport mechanism of the carriers to simulate the ensemble velocity of the charge carriers under applied external electromagnetic forces without use of any continuum model. The **TNL-TS simulator** has capabilities to simulate the hot electron transportation in the semiconductor materials. The interaction time of THz pulse with carrier is designed in such a way that at least single cycle THz pulse interact with the carriers. It uses the Monte Carlo technique which has ability to improve the "state-of-the-art" treatment of high-energy carrier dynamics. The detailed understanding of the capabilities of **TNL-TS simulator** is mentioned in the sections of the chapter 3.

2.4 Need of TNL-TS simulator

The following trends in the semiconductor industry are occurring concurrently with rapid changes in the applications of semiconductors. The competitiveness among many semiconductor manufacturers is shifting from an emphasis on technology and fabrication to a much greater emphasis on product design, architecture, algorithm, and software; i.e., shifting from technology oriented research & development to product-oriented R & D in which computers, modeling, and simulation become increasingly crucial for technology success. In market place there is no such commercial software tool available for simulation and understanding of various physics based effect to explain the ultrafast carrier dynamics under the influence of THz field. THz Researchers are use hit and trail basis experiments without knowing about various physical effects to

understand the physical mechanisms during THz spectroscopy experiments which are very expensive.

The continuum methods of describing transport in semiconductors, specifically the drift-diffusion and hydrodynamic models, which are derived from moments of the semi-classical Boltzmann Transport Equation (BTE) cannot be used for explanation of the real time THz experiments. As approximations to the BTE, it is expected that at some limit, such approaches become inaccurate, or fail completely. Also these models are able to solve steady state carrier transport mechanisms under the condition when carriers attain equilibrium distribution function. Also, the Drude model based on certain equation with fitting parameters is unable to explain low THz frequency conductivity. Indeed, one can envision that, as physical dimensions are reduced, at some level a continuum description of current breaks down, and the granular nature of the individual charge particles constituting the charge density in the active device region becomes important.

TNL-TS simulator is physics based tool, capable to extract accurate THz conductivity with the capabilities to successfully demonstrate the free carrier absorption mechanism. An overview of the technique implemented to simulate the carrier interaction with THz pulses is provided here to serve as a high-level orientation. The **TNL-TS simulator** predicts the carrier behavior on the three valleys in terms of carrier velocity. The time domain current density is computed through the current density associated with each electron in the ensemble of particles. The other ultrafast carrier's properties e.g. various scattering mechanisms rates on the three valleys over the full electronic band structure are capable to demonstrate the impact of absorbed THz photons by the electrons on the carrier motion. The atomistic physics based simulation provides three major advantages over use of continuum models;

- It accurately predict all the mechanisms even up to a single electron
- Real insight of all the mechanisms can be predicted
- It captures theoretical knowledge in a way that makes this knowledge available to non-experts.

The physics-based simulations are different from empirical modeling and through use of continuum model. **TNL-TS simulator** can help in obtaining optimum conditions and information which may be used for real time experiment calibration purposes. Also, it offers much quicker and much cheaper solutions for the validation of the experimental findings.

The algorithms of the **TNL-TS simulator** includes the solution of the seven dimensional $(x, y, z, p_x, p_y, p_z, t)$ Boltzmann transport equation with contribution of various types of scattering mechanisms. Here (x, y, z) are refer to position coordinates, (p_x, p_y, p_z) are the momentum coordinates and t is the time of order of ps. The solution is carried out to extract the carrier's nonlinear dynamics under the influence of external THz pulses.

1.3 Features of TNL-TS simulator

- Graphical User Interface (GUI) enable feature i.e. no need for coding & scripting
- User Friendly with Windows based application with full capabilities
- Powerful tool to simulates hot carrier dynamics of charged, and interacting particles
- Microscopic simulation of the motion of individual particles under the influence of the THz pulses under the influence of the internal fields of the crystal lattice and other charges, lattice defects etc
- Various types of non-linear scattering mechanisms are use to validate the real time free carrier absorption mechanism
- Information regarding dominating scattering rates responsible of material's conductivity degradation
- Fermi Golden Rule for momentum & energy conservation
- Random scattering events, particularly useful in describing inter and intraband transitions of charge carriers in bulk & nanomaterials
- Users have flexibility to initialize the carriers distribution density over many valleys or lowest energy lying valley of the material based on requirement
- Material's intrinsic noise is avoided
- Follows Aufbau principle i.e. under static field conditions most of high energy valleys carrier transfer itself to the lowest energy lying valley
- THz Pulses applications with frequencies ranging from few hundred gigahertz to several THz
- Users may trace all the carrier electronic dynamics associated with influence of THz pulses on motion even for each single electron
- Bunches of material characterization examples are inbuilt in TNL database
- Capabilities to incorporate USER'S defined new materials & its parameters easily
- TNL-TS simulator offer COST ECONOMICAL SOLUTION for calibration of THz spectroscopy based material characterization for the nano- and bulk materials

1.4 Benefits can be realized

- User Friendly with Graphical User Interface (GUI) capabilities on windows platform
- Fast and efficient algorithms with variety of material database with flexibilities to ramp USERS define THz frequencies
- Users may track all the run outputs i.e. position, momentum, energy, valley occupation etc parameters at any instant during simulation running environment
- Purely atomistic physics based modeling capabilities
- Elemental, binary and ternary compound semiconductors database available
- Ability to controlling & optimizing individual carrier transitions between different intra bands in many body states
- Extraction of the THz conductivities and absorption coefficient along with other associated parameters
- Various types of INBUILT scattering mechanisms used for calibration of experimental findings
- To avoid the transient effects that accompany the turn-on of the electric field, all time steps prior to a total elapsed time can be discarded
- State of Art tool for accurately prediction of the conductivity of a weakly confined Drude gas of electrons without using any fitting parameter

CHAPTER 2

Start using TNL-TS simulator



TNL

Blank Page

TNL

2.1 Getting Started

To use the TNL THz Spectroscopy simulator (TNL-TS simulator) user needs to get the license for this. Once they get the license for the same, they can verify it by opening the TNL-Framework. At framework user will see a tick mark on the side of the name Spectroscopy in green color which confirms the license for same as represented in figure 1 below. But if a cross mark in red color is present then user might not using valid license (in this case user needs to contact TNL Pvt. Ltd.). For more information user needs to go through the License Manual.

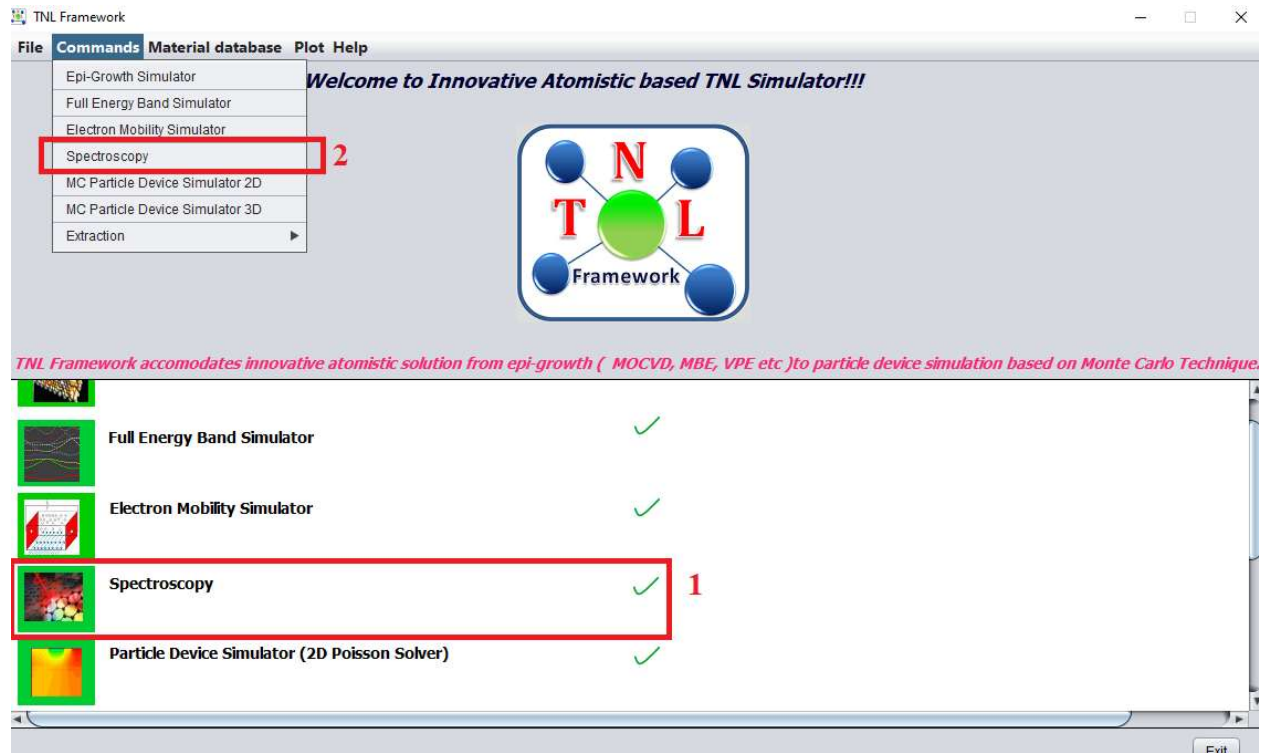


Figure 1 : TNL-Framework

There are two ways to open the TNL-TS SIMULATOR from the Framework shown in figure1. Those ways are shown in red rectangular boxes (box1 and box2).

1. This box1 contains TS Simulator's icon and name. By a single click on icon or name user gets access to use the simulator
2. This box2 contains sub menu named as Spectroscopy. By clicking on the menu Command user will get several sub-menus containing the names of all simulators of TNL family. By a single click on name user gets access to use the simulator.

Using any of the above two methods user will be directed to the TNL-TSSimulator window frame THz Spectroscopy Simulator as shown in figure2.

2.2 TNL-TS SIMULATOR window frame



Figure 2: THz Spectroscopy Simulator window frame.

TNL-TS SIMULATOR window frame in figure 2 contains several tabs named as:

1. Material
2. Mechanism
3. Output

2.2.1 Material Tab

Here several drop boxes and text fields are given containing input information regarding material, electric field, frequency, mass, permittivity, density, velocity, temperature, particles and non-parabolicity factor. We will discuss it one by one.

2.2.1.1 Choose material

- Clicking on the **Choose Material** dropbox a menu containing several materials names will be shown like shown in figure 3.
- Various semiconductor materials database is available in the simulator, e.g. Si, Ge, GaAs, InP, AlAs, InAs, GaP, GaN, InN, ZnO etc.
- Users may choose any of the material as per requirement.
- One more option available here for defining user defined ternary material by choosing User-Defined option from here. When user chooses this option a new pop-up window will open as shown in figure 4(a).

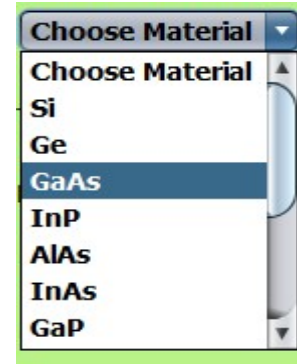


Fig 3: Choose material

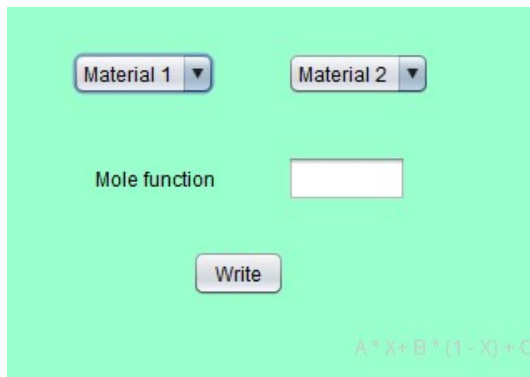


Figure 4(a)

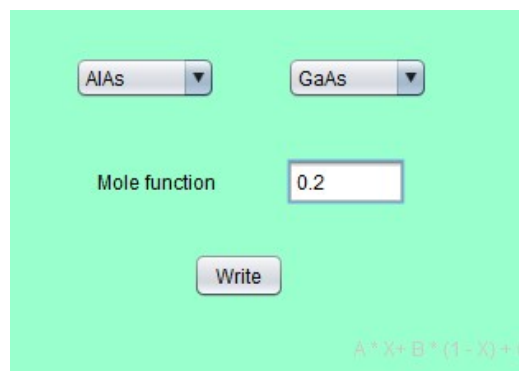


Figure 4(b)

The new pop-up window has options of material 1, material 2, mole function and write button. For example if user wants to do simulations for ternary material like $\text{Al}_{0.2}\text{Ga}_{0.8}\text{As}$ ($\text{Al}_x\text{Ga}_{1-x}\text{As}$). So they need to choose AlAs and GaAs from Material1 and Material2 options respectively. Then they need to give mole fraction value required for his defined material, 0.2 in this example. Now they have to click the “Write” button at the bottom. Users will get back to the material tab of the simulator’s frame. Here now you will see besides the choose material (User-Defined) drop-box a text-field and a “Load” button is visible. When you will click on it the text-field will show your defined material ($\text{Al}_{0.2}\text{Ga}_{0.8}\text{As}$).

The simulator is connected to the inbuilt database of the most of the semiconductor materials given here and also it will interpolate the values of the user-defined materials. So by choosing any of the materials simulator will provides those default data from database as shown in figure 5.



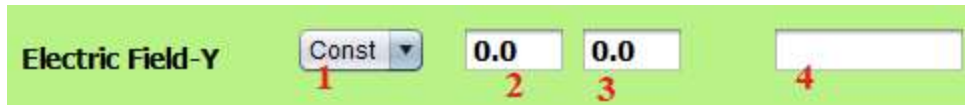
Figure 5: Default values of Ge.

While you choose a material the parameters like relative mass, permittivity, density and sound velocity of that material will be loaded automatically. All these fields values are editable, so user can input their value as per the requirement.

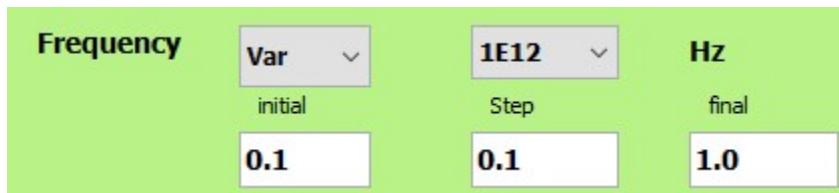
2.2.1.2 Biasing

After choosing the material, the biasing value is required to ramp the THz pulses. With the present formulation of the simulator, user needs to input the two parameters of the biasing. First is peak electric field value and second are frequency values to ramp the THz pulse. The biasing involves three values called initial, step and final. Initial value is that point at which point simulation will start first. Final value is the point upto which value the simulation will continue. Between these initial and final values, the step which means biasing will ramp from initial and final value with those step values and those are the intermediate simulation points.

Suppose user gives initial value 0, step value 0.1 and final value 1. Then the simulation will first start at the 0 then it will proceed to 0.1, 0.2, 0.3, ..., upto final value 1. During the simulation all respective output results will be saved at these step points (we will talk about it later in this tutorial). In this version we have provided vulnerability to ramp only the Frequency. In next version, users will find flexibilities to provide varying electric field also with the frequencies.

A: Electric-Field**Figure 6:** Electric- Field value

User can enter the values in the textbox fields in any direction of the the sample i.e. x, y, and z through Electric Field-X, Electric Field-Y, and Electric Field-Z. With the Electric Field-Y four options are given numbered 1 to 4 as shown in above figure. 1 is showing dropbox that contains Const (constant) as it's option in this version of simulator (*in next version we will open option for variable, so user can ramp electric field in y direction). 2,3 and 4 options are showing initial, step and final value to be inputted to ramp the electric field. In this version field 2 and 3 are kept fixed at 0kV/cm. So user needs to give the peak electric field value at field 4 as above. The unit of all electric field in x, y and z direction will be taken as kV/cm. Suppose you give value 10 in the field4 the simulator will take it as 10kV/cm.

B: Frequency**Figure 7:** Frequency value

Similarly user needs to provide the frequency values to biasing. They can give either variable or a constant frequency by choosing options Var/Const in first drop box. The second drop box contains value 1E12 Hz as we are performing simulation on sample at THz frequency. There are three fields for initial, step and final values user may provide require value similarly as per their THz experiments. If Const is chosen you need to give equal value to all these fields.

Note: *Please give your initial value equal to or greater than 0.1 for frequency.*

2.2.1.3 No. of Particles

Users may input the number of particles to initialize the simulation. These particles can be distributed over the three valleys described in section 1.2.2.2. The number of particles is contributing to the energy level calculations and further use in calculating various scattering rates. By-default 20000 particles are taken in this field; user may change this value as per their requirement. There are tradeoff between number of particles used and simulation time. More

number of particles means more accurate results. More number of particles leads to more complex and lengthy computation and can increase the simulation time.

2.2.1.4 Temp

This field represents to the temperature; at which user needs to run the simulation on the sample and they can analyze the effect of the temperature dependence of on the output results. The temperature value has been taken in unit of kelvin (K) in simulator.

2.2.1.5 Non-Parabolicity



Non Parabolicity

Γ -valley nonparabolicity

L-valley nonparabolicity

X-valley nonparabolicity

Figure 8: Non Parabolicity

Under material tab there is a check-box named Non Parabolicity, by default it is unchecked means simulator is not considering non-parabolicity effect of the energy bands. User may select it by clicking the check box, the respective values of nonparabolicity values of energy bands at various valleys of selected material will be loaded and will be shown in the fields given below named gamma, L and X valley nonparabolicity from the database.

2.2.2 Mechanism Tab

Mechanism tab contains various scattering mechanisms options and various material properties require initializing the simulation. TNL-TS simulator contains most of scattering mechanisms e.g. lattice scattering, acoustic scattering, defect scattering, carrier-carrier scattering and other scatterings.

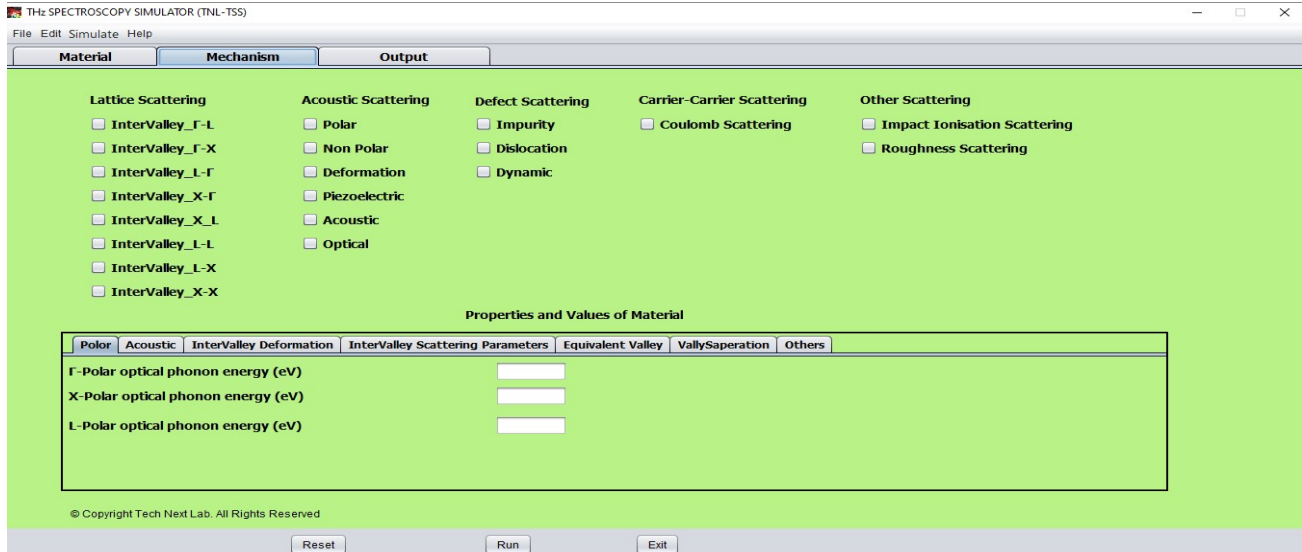


Figure 9: Mechanism frame

2.2.2.1 Scattering Mechanisms

A: Lattice scattering

It contains all intervalley scattering mechanisms

- i. Gamma to L (InterValley_Γ-L)
- ii. Gamma to X (InterValley_Γ-X)
- iii. L to Gamma (InterValley_L-Γ)
- iv. L to X (InterValley_L-X)
- v. L to L (InterValley_L-L)
- vi. X to Gamma (InterValley_X-Γ)
- vii. X to L (InterValley_X-L)
- viii. X to X (InterValley_X-X)

B: Acoustic Scattering

- i. Polar
- ii. Non-Polar
- iii. Deformation
- iv. Piezoelectric
- v. Acoustic
- vi. Optical

C: Defect Scattering

- i. Impurity
- ii. Dislocation
- iii. Dynamic

D: Carrier-carrier scattering

- i. Coulomb

E: Other Scattering

- i. Impact Ionization
- ii. Roughness

2.2.2.2 Properties and values of material

Properties and Values of Material						
Polar	Acoustic	InterValley Deformation	InterValley Scattering Parameters	Equivalent Valley	VallySaperation	Others
Γ -Polar optical phonon energy (eV)						
X-Polar optical phonon energy (eV)						
L-Polar optical phonon energy (eV)						

Figure 10: Various tab for energies value of parameters of material.

These are the important semiconductor properties used during simulation involving in scattering rates and other complex parameters calculations during carrier motion. These values are for the lattice structural, thermal, elastic, lattice dynamics, electronic energy-band structural, optical and carrier transport properties of semiconducting materials. These values play an important role in THz simulation, so user need to be careful and decisive about these parameter values.

By-default simulator loads values of the associated material of his choice as discussed in material section. (these values have been taken from various reputed literature and calibrated with experiments). However, users have flexibility to edit these values from their perspective which will be reflected in the change in output results. The parameters are shown as:

1. Polar

This tab contains polar optical phonon energies of Γ , L and X valley in eV of material.

2. Acoustic

This tab contains acoustic deformation potential of Γ , L and X valley in eV of material.

3. Intervalley Deformation

A deformation potential is a quantity proportional to a matrix element of an operator belonging to a crystal deformation between a final and initial electron state. It has the units of eV.

4. Intervalley Scattering

This tab contains phonon energy between the two valley of Γ , L and X valley in eV of material.

5. Equivalent Valley

This tab contains no. of equivalent valley for each of the Γ , L and X valleys in same Brillouin zone.

6. Valley Separation

The tab contains fields where users need to give the value corresponding to energy difference between the lower points of the two valleys. The simulator is taking gamma (Γ) valley as a reference point. So, it is required to consider the separation of X and L valley with respect to Γ valley. This separation may be a positive or a negative value depending upon the exact positions of the satellite valley with the reference Γ valley with energy value zero. The unit of this separation is in eV.

7. Others

This tab has several fields some of which are related to the scattering, some are with the doping of material and initial position of particles used in simulation.

- i. **Alloy disorder:** This is the scattering rate user need to provide when he will select the dynamic scattering from the column of defect scattering in this mechanism window.
- ii. **Line dislocation:** This is the scattering rate user need to provide when he will select the dislocation scattering from the column of defect scattering in this mechanism window.
- iii. **Ionized impurity:** This is the concentration of the impurity present in the sample material which needs to be provided when user will select the Impurity scattering from the column of defect scattering in this mechanism window.
- iv. **Piezoelectric coefficient:** This is the coefficient rate value need to provide when user will select the piezoelectric scattering from the column of acoustic scattering in this mechanism window. This coefficient is related to the volume change when a piezoelectric material is subject to the electric field or polarization on applied stress.
- v. **Doping density:** This is the doping concentration of the sample.
- vi. **Particle distribution in each valley:**

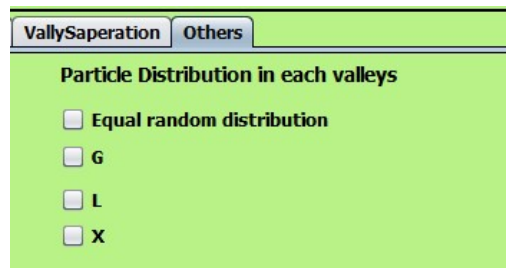


Figure11: Particle distribution

Simulator provides flexibility to the user to choose number of particles for initial distribution as described in section 1.2.1.3 to the three valleys as shown in figure11. There are four options given to do distribution like equal random distribution, Γ , L and X. If user selects equal random distribution the no. of particles initialized will be almost equally distributed with help of random technique in-built in the simulator. At this time all other three check-box will hide. If user do not select equal random distribution other three option will be available (Γ , L and X) and can choose any of these, then all particles will be initialized only in that particular valley.

In steady state condition zero field most of the particles try to occupy the lowest energy level follow the Aufbau principle. Algorithm of the simulator is designed in such a way that irrespective of the initial distribution of particles by users, particle will follow Aufbau principle and after a short time interval most of the particles residing at higher energy states will depopulated to lowest lying energy state under steady state conditions.

2.2.3 Output Tab

This tab consists of two columns named Input script i.e. the material and its parameters and scattering models chosen and the output running script.

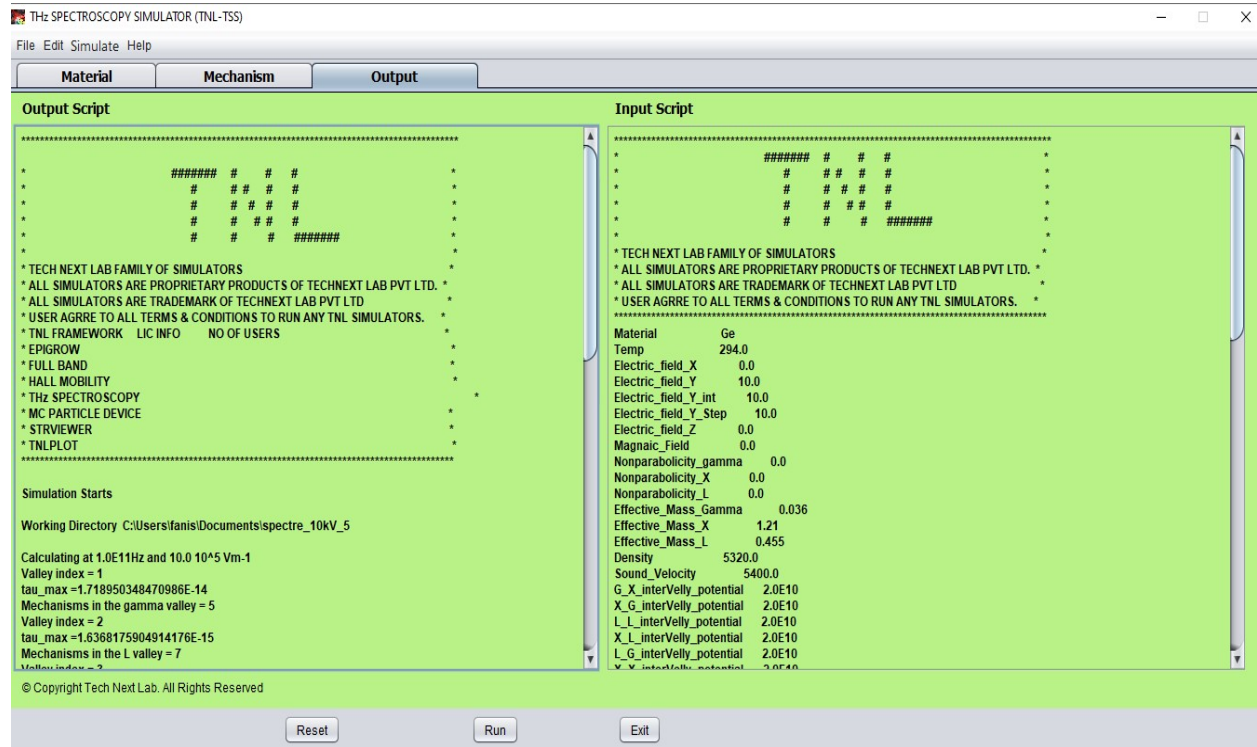


Figure 12: Output tab

1. Input script

This section shows all the input material parameter values and scattering mechanism information taken in Material and Mechanism section by the user, before clicking the “Run” button. User can check here all the input values before simulation start at this section.

2. Output script

This column will show the simulation points and its some value of each bias point. As the simulation starts it will show the directory where all the simulation results will be saved with the line named working directory. After this some value of each bias point will be shown with the line named calculating at x Hz and y V/m. At the end of last bias point it will write a line Simulation Completed which notify user the successful completion of whole simulation after that they can see the results going to the working directory of respective simulation.

2.2.4 Other Buttons

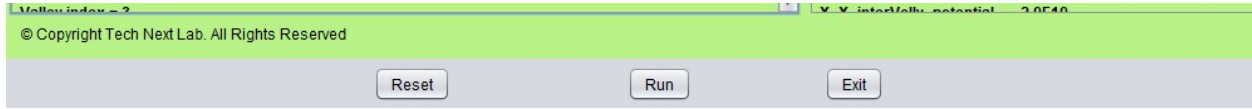


Figure 12: Other buttons

1. Run Button

To start the simulation user needs to press this Run button shown in figure 12. As user will press this button a pop window will open named save as shown in figure 13. By-default the selected directory will be 'Documents' of user computer, user can select any other directory of his computer. Then he needs to give the name of his simulation folder in the 'File Name' space and then press the 'Save' button. Thus, the working directory will be selected and all simulation will be saved in that folder.

2. Reset Button

After pressing this button all the fields in all tabs will get reset.

3. Exit Button

This button is used to exit the simulation and simulator will get close.

2.3. Hands-On Tutorial

Now we will show a hands-on demonstration of the TNL-TS simulator using knowledge of description written in above sections. The simulation of Ge material at 181kV/cm of externally applied peak electric field value at room temperature using 20000 particles equally distributed in three valleys at a time with frequency ramp from 0.1 THz to 1THz and specific scattering parameters. Use following steps:

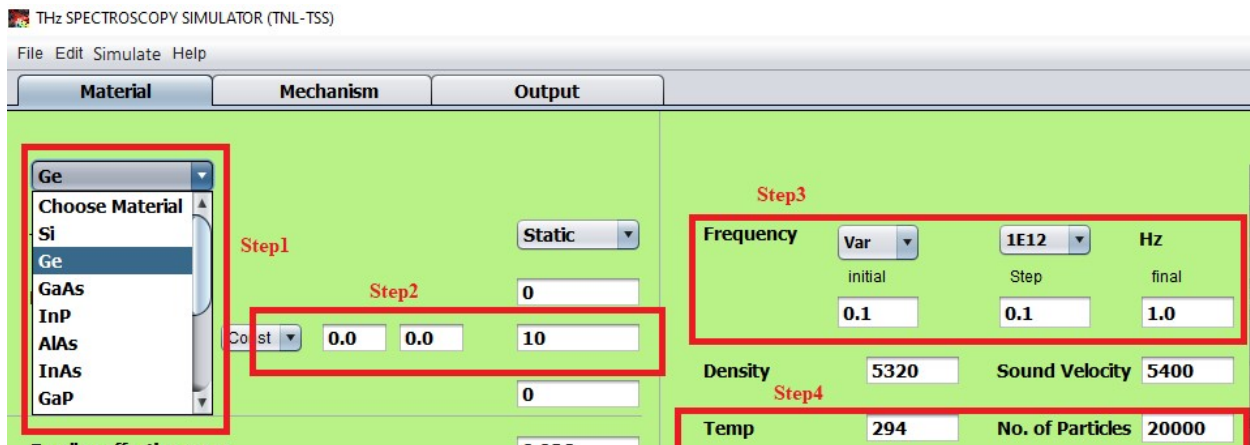


Figure 13:

Step 1: In material tab select Ge from the Choose material options. After clicking on Ge there some of the parameter will be loaded as shown in above figure 13 ins step1 red box.



Figure 14: Material tab showing five steps in red and black boxes.

Step 2: In this step as shown in Step 2 box in figure 14.

- i. Select Const.
- ii. Write 0 in Electric Field-X and Electric Field-Z.
- iii. Write 181 in final box of Electric Field-Y.

Step 3: In this step define the frequency value and type input in the bias as shown in Step 3 box shown in figure 14.

- i. Select Var.
- ii. Select 1E12 Hz.
- iii. Write 0.1 in initial, 0.1 in step and 1 in final fields.

It will vary your frequency from 0.1 to 1 THz with step of 0.1THz.

Step 4:

- i. Write 294 in Temp field.
- ii. Write 20000 in No. of Particles field.

Step 5: Define non-parabolicity value of material. Here we have not chosen in this example.

But if you want to include non-parabolicity perform following steps

- i. Select Non-Parabolicity check box.
- ii. Write non-parabolicity factor value of each valley.

Step 6: Click on Mechanism tab. Mechanism will open as shown in figure 15.

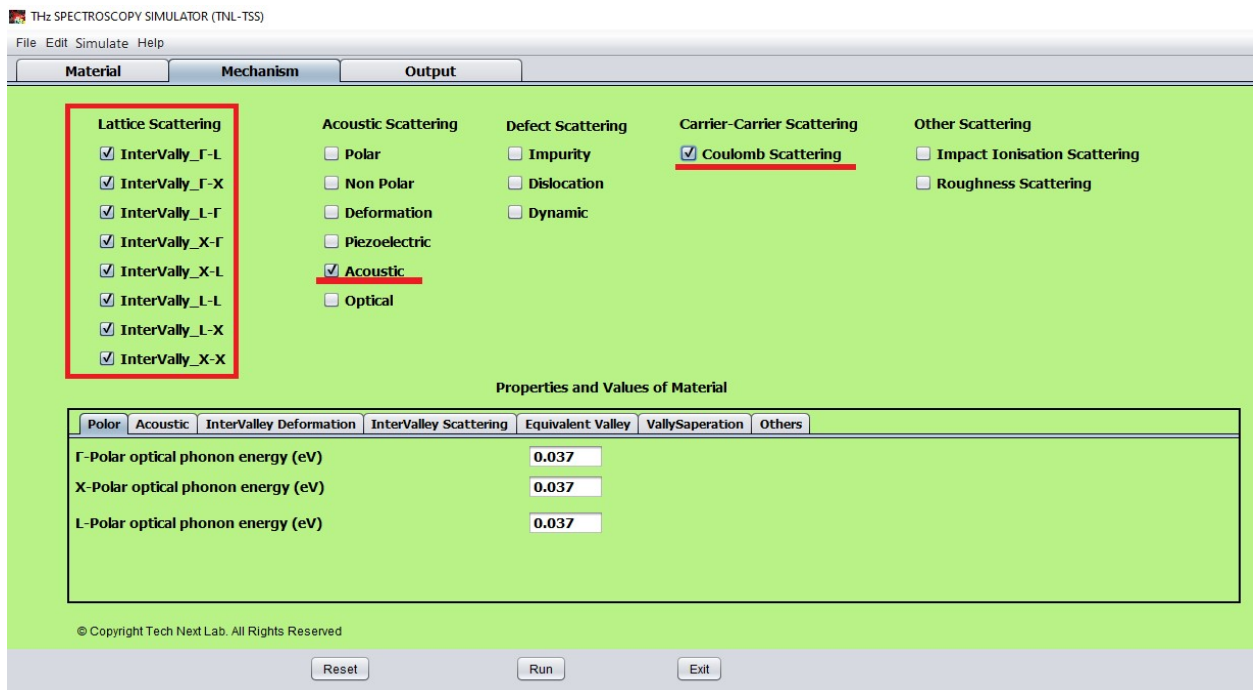


Figure 15: Mechanism tab with selected scattering mechanism (Lattice, Acoustic and Coulomb).

Step 7: As we need to select at least one scattering mechanism for successful simulation, here we have selected intervalley, acoustic and coulomb scatterings mechanisms.

Step 8: Now go to the Properties and Values of material. As we have selected the Ge material in Step1 all of the necessary values here have been pre filled. But if we need to do some modification perform following steps either skip to step 15.

Step 9: Click on Polar tab and write the required value in each field.

Step 10: Click on Acoustic tab and write the required value in each field.

Step 11: Click on Intervalley Deformation tab and write the required value in each field.

Step 12: Click on Intervalley Scattering tab and write the required value in each field.

Step 13: Click on Equivalent Valley tab and write the required value in each field.

Step 14: Click on Valley Separation and write the required value in each field.

Step 15: Click on Other tab.

Polar	Acoustic	InterValley Deformation	InterValley Scattering	Equivalent Valley	VallySaperation	Others
Alloy Disorder Scattering				0	Particle Distribution in each valleys	
Line Dislocation				0	<input checked="" type="checkbox"/> Equal random distribution	
Ionized impurity				0		
Piezoelectric Coefficient				0		
Doping density				9E22		

Figure 16:

- i. As we have not selected any of the defect scatterings and piezoelectric scattering so we will not give any value to first four fields (leave as it is).
- ii. Give doping density value 9E22 for doping of (9×10^{22} per cm^3) to the sample material chosen.
- iii. Now select Equal random distribution check box.

Step 16: Click on Output tab.

Step 17: Click on Run button. A Save pop-up window opened as shown in figure 17.

Step 18: In save window default directory is 'Documents'. Go to field named File name and write name of your file name (TNL-TS Simulator hand on for this example) to create a folder in the 'Documents' path of your system.

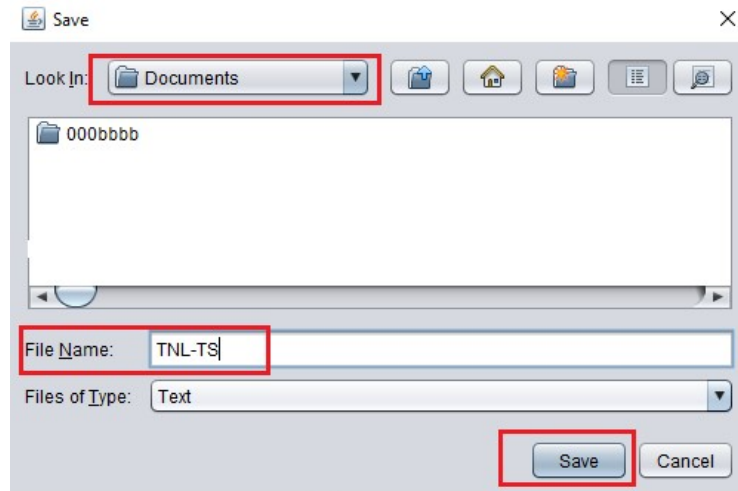


Figure 17: Save window.

Step 18: Now click Save button. With this step will start and you can see the input and output in the Input Script and Output Script of the Output tab. Output script column shows the working directory “C:\Users\...\Documents\TNL-TS”. It also shows “Calculating at 1.0E11Hz and 181 10⁵Vm⁻¹” as we have given the starting frequency 0.1*10¹² Hz.

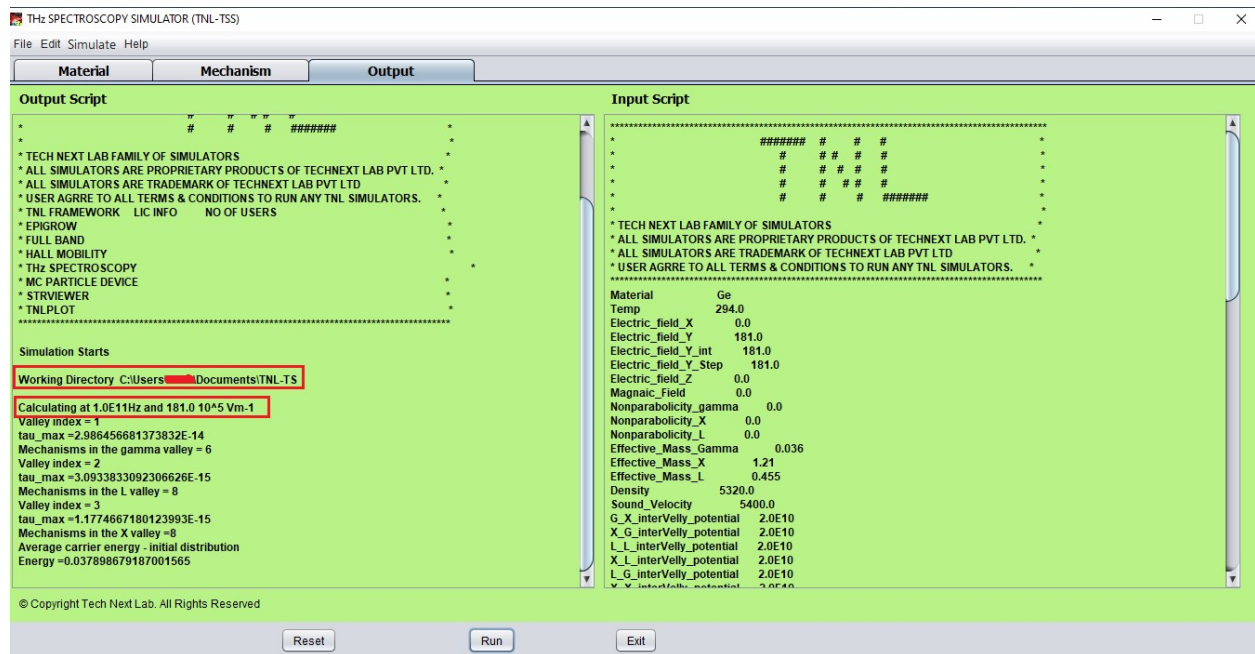


Figure 18: Output window

Step 19: Simulation will go for 0.1, 0.2, ... ,1.0 THz frequency and at last Simulation Completed message will be displayed in Output Script.

Step 20: After the completion of simulation, go to the directory you selected there is a folder named TNL-TS.

Step 21: Open this folder, there are several folder and text file as shown in figure

TNL

> This PC > Documents > TNL-TS >

Name	Date modified	Type	Size
Freq_1.0E11	2/6/2021 6:13 PM	File folder	
Freq_1.0E12	2/6/2021 6:40 PM	File folder	
Freq_2.0E11	2/6/2021 6:16 PM	File folder	
Freq_3.0E11	2/6/2021 6:18 PM	File folder	
Freq_4.0E11	2/6/2021 6:21 PM	File folder	
Freq_5.0E11	2/6/2021 6:24 PM	File folder	
Freq_6.0E11	2/6/2021 6:27 PM	File folder	
Freq_7.0E11	2/6/2021 6:30 PM	File folder	
Freq_8.0E11	2/6/2021 6:33 PM	File folder	
Freq_9.0E11	2/6/2021 6:37 PM	File folder	
plot	2/6/2021 6:13 PM	File folder	
TNL-TS	2/6/2021 6:13 PM	Text Document	5 KB

Figure 19: Output folder.

- i. In this folder you get folder at each frequency bias point named Freq_1.0E11 etc. , plot and a text file named TNL_TS. Each bias point folder contains a folder named E_field_181.0kV. Open this field folder which contains various file related to the simulation.
- ii. So, we will get all the information of th Ge material our applied electric field in y-direction at each frequency point.
- iii. Open any of these folders we will get files related to the scatterings selected, like acoustic, coulomb and intervalley for each valley. These contain scattering rates with respect to the energy levels.
- iv. Valley occupation files containing valley population at any time instant at that particular frequency.
- v. L, X and Gamma renormalized table value.
- vi. Velocity time averages in x, y and z direction.
- vii. Electric field vs time file at that particular frequency.
- viii. In plot folder the outputs data of simulation are
 - 1) current_density_vs_time,
 - 2) velocity_vs_time,
 - 3) Frequency_vs_Absorption,
 - 4) Frequency_vs_Conductivity,
 - 5) L-plot,
 - 6) X-plot and
 - 7) Gamma-plot.
- ix. We can plot these results on **TNL-PLOT** by importing the data file.
- x. The text file contains all the input parameter given to the simulator.

CHAPTER 3

Physics



Blank Page

TNL

3.1 Introduction

TNL-TS (THz Spectroscopy) simulator predicts the hot carrier dynamics through solution of Boltzmann transport equation (BTE) coupled with non-linear scattering mechanisms in phase space without using any fitting parameters. The carrier dynamics in the semiconductor materials at a given temperature is simulated under the influence of the varying frequencies THz pulses. The interaction time of THz pulses with carriers are chosen such that at least single cycle THz pulse from the applied continuous THz pulses may pass through the semiconductor sample during a single complete iteration. The THz field strength is responsible to disturb the steady state conditions e.g. carrier distribution function, carrier mean energy, valley carrier population ratio, carrier's average drift velocity along with the impact of various types of nonlinear scattering mechanisms. The carrier distribution function follows the Fermi-Dirac (FD) statistics under equilibrium conditions i.e. steady state conditions when no external forces are acting over them. The application of THz pulses perturbs the equilibrium condition and carrier distribution function no more shows resemblance with the Fermi-Dirac (FD) function. The interaction of THz photons with carriers, the carrier distribution function is decided by the nonlinear carrier dynamics on three valleys over full band structure. The contribution of the interaction among ensemble of carriers and between the carriers to host crystals, also play significant role in estimation of the nonlinear carrier dynamics. The carrier dynamics is recorded after the excitation followed by the THz energy absorption by the carriers. TNL-TS simulator helps to validate the real time THz conductivity experimental results through extracting the free carrier absorption spectra with capabilities to successful demonstrate the ultrafast carrier dynamics with physics based phenomenon at atomistic scale.

The TNL-TS simulator is capable to extract the hot carrier velocities and other transport properties without using any fitting parameter. The carrier distribution function contains lot of valuable information associated with each carrier under non-equilibrium conditions. The Boltzmann transport equation (BTE) is able to predict accurately the hot carrier dynamics under the influence of THz field strength. However, the numerical technique for the solution of the 6-dimensional integro-differential form of BTE equation usually makes it necessary to introduce rather severe approximations, particularly when non-randomizing, inelastic collisions are taken into the consideration.

The Monte Carlo (MC) method is a best suited method for the solution of BTE coupled with nonlinear scattering mechanisms. The method considers the physical model adopted for the

TNL

scattering rates which are dependent on the material properties over the full electronic band structure. The generalized MC method is developed for the solution of BTE to incorporate the complicated scattering processes associated with ensemble of the carriers for the scan of each and every carrier over band structure of the material during any time instant of simulation with great ease [1] – [3].

The scope of the ensemble Monte Carlo (EMC) method for the estimation of the ultrafast carrier dynamics through simulation is simply extended to include the case where transient THz pulses are present. It is then possible to calculate, the time dependent conductivities. By using Fourier transform equations to convert the time dependent parameters into frequency dependent parameters of the semiconductor material as a function of THz frequencies [4]. The non-equilibrium time evolution of carriers and low-energy excitations within sub- picoseconds (ps) time resolution due to the interaction with the THz photons involves several additional complications. The formulation of charge carrier dynamics on the electronic band structure is *beyond the equilibrium transport conditions*. The structure and size of material itself dictate and decide the physics of the collision processes due to the presence of localized phonons, interfacial excitations etc.

The prior knowledge of full electronic band structure of the semiconductor is an essential requirement to start with the THz spectroscopy simulation. The TNL-FB simulator is capable to simulate full electronic band structure using empirical pseudopotential method (EPM). The details of method and simulator are given in the manual of TNL-FB simulator. The capabilities of the TNL-FB simulator shows that qualitatively and, often, quantitative accurate results are obtained in a variety of systems of interest such as thick / thin semiconducting (group VI, IV-IV, III-V and II-VI) bodies. The reasons for focusing on ‘empirical’ pseudopotentials are twofold: first, users may develop a general scheme based on accurate k-space band-structure methods which leads to the solution of electronic quantum transport in semiconductor material under the THz fields. Electrons in a perfect crystal is described in terms of Bloch states, whose wave functions are written as

$$\psi_{nk}(r) = u_{nk}(r)e^{ik \cdot r} \quad (3.1)$$

where n is a band index, $\hbar k$ is the quasi momentum of the electron with k wave vector, and $u_{nk}(r)$ is a function of the space coordinate ‘r’ with the periodicity of the crystal.

For each band n , a value of the electron energy $\varepsilon_n(k)$ is associated to the electronic state k . The set of functions $\varepsilon_n(k)$ describes the band structure of the semiconductor material. The uses of plane waves and pseudopotentials to calculate the band structure of semiconductors have proven useful technique to gain insight into the electronic excitation spectrum of the solids. The ‘empirical’ nature implies loss of strong predictive power and ‘portability’ of ionic (pseudo) potentials, but it results in a vast simplification of the numerical problem in comparison to the various ab-initio methods based techniques. The small degree of fitting in EPM allowed by the technique which affords by definition and excellent agreement is obtained with the experimental data. Since our focus is on ultrafast electronic transport, not on structure calculations, it represents the best choice to perform accurate calculations of various physical parameters. The knowledge of the band structure of a solid is the starting point for the study of any electronic property associated with hot carrier dynamics. The full band structure of the thin / thick films can be simulated with *TNL-FB (FullBand)* simulator. The details of band structure calculation are given in user manual of *TNL-FB (FullBand)* simulator.

3.2 Hot Carrier Transportation

The *TNL-TS (THz Spectroscopy)* simulator includes an innovative technique applied for accurate predictions of the hot carrier dynamics properties. It is capable to simulate the free particle motion on the three valleys over full band structure refer to as the free flight of the carrier and terminated by instantaneous random scattering events. The solution of Boltzmann transport equation (BTE) through Monte Carlo (MC) method consists of generating random free flight times for each particle, choosing the types of scattering processes based on specific material, occurring at the end of the free flight. The scattering events change the final energy and momentum of the particle after the scattering mechanism, and then repeating the same procedure for the next free flight. The sampling of the carrier motion at various time steps throughout the simulation allows for the statistical estimation of physically interesting quantities such as the carrier distribution function, the average carrier drift velocity under varying THz fields and frequencies strengths, the average energy of the particles, *etc.* By simulating an *ensemble* of particles, representative of the physical system of interest, the non-stationary time-dependent evolution of the electron distributions under the influence of a time-dependent driving force arises due to THz field. *TNL-TS simulator*, the particle picture can be realized where the carrier motion is decomposed into free flights terminated by instantaneous collisions. It is basically the

similar predictive picture underlying the derivation of the semi-classical Boltzmann transport equation (BTE).

The Boltzmann transport equation (BTE) can be characterized by a region of phase space about the points (x, y, z, p_x, p_y, p_z) . The number of particles entering into this region in time dt is equal to the number of particles which were in the region of phase space $(x-v_x dt, y-v_y dt, z-v_z dt, p_x-F_x dt, p_y-F_y dt, p_z-F_z dt)$ at a time dt earlier. Here F represents the applied force field, v_i are the carrier velocity and p_i are the carrier momentum in the respective directions.

In case, the distribution function $f(x, y, z, p_x, p_y, p_z)$ expresses the number of particles per quantum state in the region, then the change in the distribution function df which occurs during time dt due to the change the carrier's wave vector in the coordinate space under the influence of the THz pulses. The force fields due to THz photons acting on the carriers, tend to move them from one region to another in momentum space is [5] – [10] and can be described as;

$$df = f(x - v_x dt, y - v_y dt, z - v_z dt, p_x - F_x dt, p_y - F_y dt, p_z - F_z dt) - f(x, y, z, p_x, p_y, p_z) \quad (3.2)$$

Using Taylor series expansion, we get

$$\frac{df}{dt} = -\mathbf{v} \cdot \nabla_r f - \mathbf{F} \cdot \nabla_p f \quad (3.3)$$

Equation (3.3) represents only the change in the distribution function due to the motion of carriers in coordinate space and due to the momentum changes arising from the external THz force fields acting on the electrons. Electrons are also be transferred into or out of a given region in the phase space through the collisions or scattering interactions involving other particles of the distribution or scattering centers external to the assembly of particles under consideration. If the rate of change of the distribution function due to collisions, or scattering, is denoted by the function $(\partial f / \partial t)_{coll}$, the total rate of change of f becomes

$$\frac{df}{dt} = -\mathbf{v} \cdot \nabla_r f - \mathbf{F} \cdot \nabla_p f + \left. \frac{\partial f}{\partial t} \right|_{collision} \quad (3.4)$$

Rearranging equation (3.4),

$$\frac{df}{dt} + \mathbf{v} \cdot \nabla_r f + \mathbf{F} \cdot \nabla_p f = \left. \frac{\partial f}{\partial t} \right|_{collision} \quad (3.5)$$

Eq. (3.5) represents the Boltzmann transport equation with capabilities to handle the particle flow in the phase space. The various terms in eq. (3.5) is describing below.

The last term on the LHS of eq. (3.5) represent the carrier motion under applied THz force field and is given as;

$$\left(\partial f / \partial t\right)_{forces} = -\mathbf{F} \cdot \nabla_{\mathbf{p}} f, \quad (3.6)$$

The total force field \mathbf{F} is equal to the sum of the forces acting over the carriers due to the externally applied field and is given as

$$F = qE \quad (3.7)$$

THz force field \mathbf{E} and is given as,

$$E = E_0 \cos(2\pi f n dt) \quad (3.8)$$

Here, E_0 is the peak amplitude of the driving THz pulse, f is the THz pulse frequency, n is the number of total time steps and dt is the time step between two successive events i.e. simply known as the duration of the carrier interaction. The product $n \cdot dt$ is the total interaction time of the field. The time of interaction of the THz pulses with the carrier are chosen in terms of interaction time 'dt'. In *TNL-TS simulator*, the value of 'dt' is chosen in such a way that at least a single cycle of the THz pulse from the applied continuous THz pulse interact with the carriers in the sample during one complete iteration with the condition $f = \frac{1}{T} \geq 0.01$, T is the time period of the mono-frequency THz pulse. It is clear that increase in the THz pulse frequencies the time period decreases. The interaction time of THz pulse with the carriers decreases. The successive various THz mono-frequency pulses interact with the carriers. The single cycle THz pulse is passed through semiconductor sample for every THz frequency pulses with the condition $f \geq 0.1$ THz, during one complete iteration.

The applied THz force field responsible for carrier motion in the phase space, is written as

$$F = \frac{dp}{dt} = \hbar \frac{dk}{dt} \quad (3.9)$$

Combining eq. (3.7) and (3.9) the force on each particle can be computed.

The second term on the LHS of Eqs. (3.5) is given as

$$\left(\partial f / \partial t\right)_{diff} = -\mathbf{v} \cdot \nabla_{\mathbf{r}} f \quad (3.10)$$

The above term represents a spatial variation of the carrier distribution function due to concentration or temperature gradients, both of which are result in a diffusion of carriers in the coordinate space.

The first term on the RHS of Eqs. (3.5), $(\partial f / \partial t)_{coll}$ represents the collision or scattering term. It is computed with the difference between the carrier in-scattering and the out-scattering processes, and is estimated as

$$\left(\frac{\partial f}{\partial t} \right)_{coll} = \sum_{k'} \{ S(\mathbf{k}', \mathbf{k}) f(\mathbf{k}') [1 - f(\mathbf{k})] - S(\mathbf{k}, \mathbf{k}') f(\mathbf{k}) [1 - f(\mathbf{k}')] \} = \widehat{C}f \quad (3.11)$$

Here, $\frac{1}{\tau(k)} = \sum S_i(k, k')$ is the total scattering rate out of state k . The presence of $f(\mathbf{k})$ and $f(\mathbf{k}')$ in the collision integral makes the BTE rather complicated integro-differential equation for the solution of distribution function $f(\mathbf{r}, \mathbf{k}, t)$, whose solution requires a number of simplifying assumptions. In the absence of perturbing fields and temperature gradients, the distribution function must be followed the Fermi-Dirac distribution function. Under this condition, the collision term must vanish and the principle of detailed balance method gives for all \mathbf{k} and \mathbf{k}' and all scattering mechanisms

$$\frac{S(\mathbf{k}, \mathbf{k}')}{S(\mathbf{k}', \mathbf{k})} = \frac{f_0(\mathbf{k}') [1 - f_0(\mathbf{k})]}{f_0(\mathbf{k}) [1 - f_0(\mathbf{k}')]}. \quad (3.12)$$

Therefore, if the phonons interacting with the electrons are in thermal equilibrium, we get

$$\frac{S(\mathbf{k}, \mathbf{k}')}{S(\mathbf{k}', \mathbf{k})} = \exp\left(\frac{E_{\mathbf{k}} - E_{\mathbf{k}'}}{k_B T} \right). \quad (3.13)$$

This relation must be satisfied regardless of the origin of the scattering forces. In case for example, if we assume $E_{\mathbf{k}} > E_{\mathbf{k}'}$, then $S(\mathbf{k}, \mathbf{k}') > S(\mathbf{k}', \mathbf{k})$ i.e. phonon emission rate must exceed absorption rate. Note that the BTE is valid under assumptions of semi-classical transport: effective mass approximation (which incorporates the quantum effects due to the periodicity of the crystal); Born approximation for the collisions, in the limit of small perturbation for the electron-phonon interaction and instantaneous collisions; no memory effects, i.e. no dependence on initial condition terms. The phonons are usually treated as in equilibrium, although the condition of non-equilibrium phonons may be included through an additional equation.

3.3 Scattering Mechanisms

The total scattering rate Γ_j is a sum of all possible scattering rates. In the *TNL-TS* simulator for computational technical reasons, each scattering mechanism has been numbered sequentially from one to N_r . Users have no need to worry about the numbering of scattering mechanisms

which *TNL-TS* simulator decide itself and cannot be changed during running simulation. the total number of such scattering mechanisms contribute based on various material properties. The total scattering rate is given as;

$$\Gamma[\mathbf{k}(t)] = \sum_{i=1}^{N_r} \lambda_i[\mathbf{k}(t)] \quad (3.14)$$

where t represents time, which is related to the energy or wave vector of the scattering particle through eq. (3.14), and λ_i the rate of i^{th} scattering mechanism. The scattering mechanisms are responsible of terminating the free flight which is selected by means of a random number.

$$r_\gamma = \Gamma r_s \quad (3.15)$$

where r_s represents a random number.

Free carrier (electrons) gain energy by absorption of THz photon energy and interact with the crystal lattice and with each other through a variety of scattering processes. Based on first order, time-dependent perturbation theory the transition rate from an initial state \mathbf{k} in band n to a final state \mathbf{k}' in band m for the j^{th} scattering mechanism govern by Fermi's Golden rule [11].

3.3.1 Fermi's Golden Rule

The scattering rate per unit time of a carrier in state $\Psi_n(\mathbf{k}, \mathbf{r})$ to a state $\Psi_n(\mathbf{k}', \mathbf{r})$ due to a first-order perturbation of the Hamiltonian from H to magnitude H' can be estimated from time dependent perturbation theory and is given as

$$S(k', k) = \frac{2\pi}{\hbar} |\langle k' | H' | k \rangle| \delta(\varepsilon_{k'} - \varepsilon_k \mp \hbar\omega) \quad (3.16)$$

where the Dirac bra and ket variables \mathbf{k} and \mathbf{k}' denote the corresponding state wave vectors. The Kronecker delta function 'δ' in (3.16) is the factor which enforces the conditions of the conservation of energy between the initial and final energy states i.e. ε_k and $\varepsilon_{k'}$, respectively accounting for the emission or absorption of a phonon of energy $\hbar\omega$ during the scattering process, where \hbar is the Planck constant and ω denotes the phonon frequency. The famous energy conservation principle represented by eq. (3.16) is known as the Fermi Golden Rule. It assumes that momentum scattering occurs instantaneously, and the real-space position of the particle remains constant during the collision. The particular form of Hamiltonian H' depends on the relevant scattering mechanism under consideration for the specific material of interest. Furthermore, the form of the Bloch function as given by (3.1) needs to modify, in case the motion of the particle is dimensionally restricted due to the carrier quantum confinement effect in a particular direction in the semiconductor material. The total scattering rate is given as;

$$\Gamma_j[n, \mathbf{k}; m, \mathbf{k}'] = \frac{2\pi}{\hbar} \left| \langle m, \mathbf{k}' | V_j(\mathbf{r}) | n, \mathbf{k} \rangle \right|^2 \delta(\varepsilon_{\mathbf{k}'} - \varepsilon_{\mathbf{k}} \mp \hbar\omega) \quad (3.17)$$

where $V_j(\mathbf{r})$ is the scattering potential of this process, ε_k and $\varepsilon_{k'}$ are the initial and final state energies of the particle. The delta function describes conservation of energy, valid for long times after the scattering event is over, with $\hbar\omega$ the energy absorbed (upper sign) or emitted (lower sign) during the process. The total scattering rate used to generate the free flight is given by

$$\Gamma_j[n, \mathbf{k}] = \frac{2\pi}{\hbar} \sum_{m, \mathbf{k}'} \left| \langle m, \mathbf{k}' | V_j(\mathbf{r}) | n, \mathbf{k} \rangle \right|^2 \delta(\varepsilon_{\mathbf{k}'} - \varepsilon_{\mathbf{k}} \mp \hbar\omega) . \quad (3.18)$$

The scattering rates $\Gamma_j[n, \mathbf{k}; m, \mathbf{k}']$ and $\Gamma_j[n, \mathbf{k}]$ are calculated using time dependent perturbation theory using Fermi's rule, eqn. (3.17) and (3.18), and the calculated rates are then tabulated in a scattering table in order to select the type of scattering and final state after scattering as discussed above in this chapter. That scattering mechanism j is selected satisfying the inequality from the eqn. (3.14):

$$\sum_{i=1}^{j-1} \lambda_i[k(t)] \leq r_\gamma < \sum_{i=1}^j \lambda_i[k(t)] \quad (3.19)$$

with

$$\sum_{i=1}^0 \lambda_i[k(t)] = 0 \quad (3.20)$$

Thus, the various scattering mechanisms are passed through in the sequence and they have been ordered until $\sum \lambda_i$ exceeds r_γ . The search terminates sooner the smaller the value of r_γ , *TNL-TS* simulator is equipped with the above-mentioned method for selection of numbering of the various scattering mechanisms. This scheme makes a weighted selection such that, over a long period of time, the relative amount of scattering from a particular type equals its fractional part of the total scattering rate or cross-section. The details of various types of scattering mechanisms implemented in the *TNL-TS* simulator are given below [3], [7].

The basic formalisms used in *TNL-TS* simulator for accounting the contribution of the various types of scattering events are as above:

- Fraction of all scattering events caused by polar optical phonons against the THz field for each separate minimum.

e = phonon emission

a = absorption

- Fraction of all scattering events during steady state causing transfer of carriers between conduction band minima in semiconductor materials against the THz force field.

Carrier intervalley transitions between three valleys (Γ, L, X) in **Zincblende** structure symmetry in forward and reverse directions are considered as;

$\Gamma \rightarrow X, L \rightarrow X$ and $\Gamma \rightarrow L$ & $X \rightarrow \Gamma, X \rightarrow L$ and $L \rightarrow \Gamma$ valleys

Carrier intervalley transitions between three valleys (Γ, Γ_3, U) in **Wurtzite** structure symmetry are considered as;

$\Gamma \rightarrow U, U \rightarrow \Gamma_3$ and $\Gamma \rightarrow \Gamma_3$ & $\Gamma_3 \rightarrow \Gamma, \Gamma_3 \rightarrow U$ and $U \rightarrow \Gamma$ valleys

with

e = phonon emission

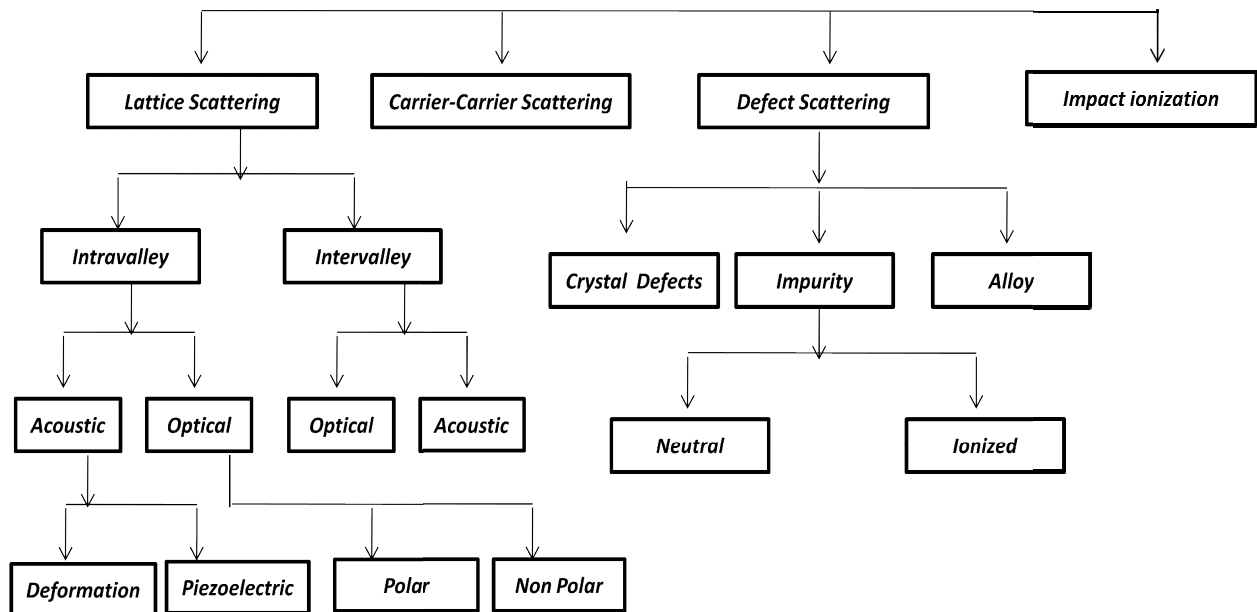
a = absorption

- Fraction of scattering events during steady state conditions causing transfer within the equivalent X & Γ_3 and L & U minima in zincblende & wurtzite semiconductor materials respectively.

e = phonon emission

TNL

$a = \text{absorption}$



Scattering mechanisms in a typical semiconductor implemented in THz Spectroscopy simulator

The collision term in the Boltzmann transport equation defines the internal relaxation mechanisms for the carriers, which are related to the collision of charged carriers (electrons) with different scattering sources (e.g., scattering of electrons by acoustical phonons and ionized impurity etc) in a semiconductor under the influence of external THz force field. These scattering mechanisms are responsible for the charged carriers to reach at steady-state conditions. In other words, under the application of external forces, the carriers start free flight from steady state condition and follow the transient state conditions, and return to equilibrium conditions when external forces are removed. The elastic scattering mechanisms include the non equilibrium distribution function which decay exponentially with the time. The time constant associated with this exponential decay is known as the collision time.

Several important scattering mechanisms as depicted above, such as acoustical phonon and optical phonon scatterings, ionized impurity scattering, and neutral impurity scattering, Coulomb scattering and defects scattering etc. play a significant role in determining the carrier drift velocity, current density and conductivities of the material.

The standard scattering processes' following Fermi's Golden Rule are implemented in the TNL-TS simulator and are given below. There is flexibility for users to use any or more scattering

processes appropriate for different semiconductor materials during validation of the experimental conductivity results. Using quantum-mechanical treatments, the scattering mechanisms have been derived in the following section.

a. Lattice scattering

1. Intravalley
 - i. Acoustic (Deformation and Piezoelectric)
 - ii. Optical (Polar and Non-polar)

b. Defect scattering:

1. Impurity
2. Alloy
3. Dislocation

c. Piezoelectric

d. Carrier-carrier scattering

e. Impact Ionization

f. Surface Roughness

3.3.2 Acoustic Deformation Potential Scattering

The acoustic phonons are responsible for the maximum energy transfer during an electronic interaction. In acoustic scattering process, the phonons energies are much smaller than the electron energy, and thus the acoustic scattering is treated as an elastic scattering process. Acoustic scattering pave way to understand the exchange of an infinitesimal amount of energy between the electrons and the crystal. Under high temperatures or high field conditions, the average electron energy is larger than the optical-phonon energy and this kind of phonon will be responsible for the task of exchanging energy between the electrons and the crystal.

As mentioned in section (3.1), the physical quantity of interest is the interaction potential resulting from the induced strain. Hence,

$$H'(\mathbf{r}, t) = \Xi_{ac} \nabla \cdot \mathbf{u}(\mathbf{r}, t) \quad (3.21)$$

where Ξ_{ac} denotes the acoustic deformation potential and $\mathbf{u}(\mathbf{r}, t)$ is given as

$$\mathbf{u}(\mathbf{r}, t) = \sum_{\mathbf{q}} \left(\frac{\hbar}{2\rho\Omega} \right)^{\frac{1}{2}} \mathbf{e}_{\mathbf{q}} (a_{\mathbf{q}} + a_{-\mathbf{q}}^{\dagger}) e^{i\mathbf{q}\cdot\mathbf{r}} \quad (3.22)$$

Here \mathbf{q} is all phonon wave vectors (modes) summation and $\omega_{\mathbf{q}}$ is the angular frequency, Ω is the crystal volume, $\mathbf{e}_{\mathbf{q}}$ is the unit polarization vector, and $a_{-\mathbf{q}}^{\dagger}$ and $a_{\mathbf{q}}$ are the quantum mechanical raising and lowering operators, respectively.

At $T=300\text{K}$, the energy $\hbar\omega \ll k_{\text{B}}T$, assuming the equi-partition approximation $N_o(\omega_o) = \frac{k_{\text{B}}T}{\hbar\omega}$ so that $N_o(\omega_o) = N_o(\omega_o) + 1$ and $\hbar\omega \approx 0$. The acoustic scattering rate is

$$\Gamma(\varepsilon_k) = \frac{2\pi\Xi_{ac}^2 k_{\text{B}}T}{\hbar c_l} N(\varepsilon_k) \left(\frac{(1+\alpha\varepsilon_k)^2 + \frac{1}{3}(\alpha\varepsilon_k)^2}{(1+2\alpha\varepsilon_k)^2} \right) \quad (3.23)$$

where T is the lattice temperature, c_l is the material dependent elastic constant dependent on the mass density ρ and velocity of sound in material v_s and defined as

$$c_l = \rho v_s^2 \quad (3.24)$$

The density of states, $N(\varepsilon_k)$ for a carrier in a non-parabolic band is given as

$$N(\varepsilon_k) = (2m^*)^{\frac{3}{2}} \gamma^{\frac{1}{2}}(\varepsilon_k) \frac{d\gamma(\varepsilon_k)}{d\varepsilon_k} \quad (3.25)$$

where function γ is dependent on the energy.

$$\gamma(\varepsilon_k) = \varepsilon(1 + \alpha\varepsilon) = \frac{\hbar^2 k^2}{2m^*} \quad (3.26)$$

For a parabolic, ellipsoidal band, density of states mass m_d can be written as;

$$m_d = (m_l m_t^2)^{1/3} \quad (3.27)$$

The acoustic deformation potential scattering is isotropic for spherical and parabolic bands. The final wave vector can be chosen at random since all scattering angles are equally probable. In the case of non-parabolic bands, the scattering is not strictly isotropic.

3.3.3 Non-Polar Optical Scattering

The optical phonons are assumed to remain at constant equivalent temperature as the dispersion relation of such kind of phonons is observed quite flat for the q values involved in electronic intravalley transitions. This kind of scattering is isotropic and dependent on the interaction potential, which is proportional to the displacement as compared to the case of acoustic deformation potential scattering where induced strain is of importance. The phonon energies at higher optical frequencies are of the order of the thermal energy involved in these interactions.

Therefore, for non-polar optical phonons near the zone center the interaction potential is given as

$$H'(\mathbf{r}, t) = D_{ij} \cdot \mathbf{u}(\mathbf{r}, t) \quad (3.28)$$

Here D_{ij} is a valley dependent deformation potential

At near to the edges of the Brillouin zone, the non-polar optical phonons that contribute to intervalley scattering are at slightly lower energies (on the order of a few meV) than those at the zone center.

$$\Gamma(\varepsilon_{\mathbf{k}}) = \left(\frac{\pi D_{ij}^2 Z_j}{\rho \omega_{ij}} \right) \left(N_o(\omega_o) + \frac{1}{2} \mp \frac{1}{2} \right) \left(\frac{(2m_d)^{3/2} \sqrt{\varepsilon_f(1+\alpha\varepsilon_f)}}{4\pi^2 \hbar^3} \right) (1 + 2\alpha\varepsilon_f) \quad (3.29)$$

$$\text{with,} \quad \varepsilon_f = \varepsilon_{\mathbf{k}} \pm \hbar\omega_{ij} - \Delta\varepsilon_{ij} \quad (3.30)$$

where, $\Delta\varepsilon_{ij}$ and ω_{ij} denote the energy offset and intervalley phonon frequency, respectively, between the i^{th} and j^{th} valleys in the 3-valley model employed. Z_j denotes the number of equivalent j valleys due to crystal symmetry and ρ is the mass density.

3.3.4 Polar Optical Phonon Scattering

The electrostatic nature of the interaction is strongly anisotropic in nature. The treatment of this scattering is again simplified by the constancy of the phonon energy in the transition similar to *Non-Polar Optical Scattering*. At high electron energies the total scattering rate for polar optical scattering decreases with increasing energy, owing to the electrostatic nature of the interaction. The scattering rate is

$$\Gamma(\varepsilon_k) = \left(\frac{\sqrt{m_d} e^2 \omega_{LO}}{4\sqrt{2}\pi\hbar\epsilon_p} \right) \left(N_o + \frac{1}{2} \mp \frac{1}{2} \right) \left(\frac{1+2\alpha\varepsilon_{k'}}{\gamma(\varepsilon_k)} \right) F(\varepsilon_k, \varepsilon_{k'}) \quad (3.31)$$

With,

$$N_o = \frac{1}{e^{\hbar\omega_{LO}/k_B T} - 1}, \quad \frac{1}{\epsilon_p} = \frac{1}{\epsilon_{high}} - \frac{1}{\epsilon_{low}} \quad (3.32)$$

and
$$F(\varepsilon_k, \varepsilon_{k'}) = \frac{\sqrt{\gamma(\varepsilon_k)} + \sqrt{\gamma(\varepsilon_{k'})}}{\sqrt{\gamma(\varepsilon_k)} - \sqrt{\gamma(\varepsilon_{k'})}} \quad (3.33)$$

Here, ω_{LO} is the longitudinal optical phonon frequency, m_d is density of states mass, ϵ_{high} and ϵ_{low} are the high frequency and low frequency dielectric constant of the material. $\gamma(\varepsilon_k)$ is defined as a function dependent upon nonparabolicity of the bands.

3.3.5 Ionized Impurity Scattering

In highly doped semiconductors (doping density greater than $\sim 10^{23}/\text{m}^3$), the resulting ionized impurities create coulombic potentials that scatter the carriers. These potentials are screened by the free carriers in the vicinity of the ions. A screening model similar to Brooks-Herring model is used in *TNL-TS* simulator. This type of collisions is elastic in nature and therefore it cannot alone control the transport process in the presence of an external field. It must be accompanied by some other dissipating scattering mechanism if the proper energy distribution of electrons is to be derived from theory. Owing to the electrostatic nature of the interaction, the efficiency of ionized impurity scattering decreases as the temperature of the crystal increases. In *TNL-TS* simulator, the screened perturbation potential is given by

$$V(r) = \frac{Zen_o}{4\pi\epsilon_s r} e^{-q_D r} \quad (3.34)$$

where Ze is the total charge of the ions, r the distance of the carrier from the ion, and n_o is the equilibrium density (i.e., the density of free carriers that would exist in the vicinity of the impurity if it were not ionized). The screening factor, q_D , is taken as the Debye wavevector given by

$$q_D = \sqrt{\frac{e^2 n_o}{\epsilon_s k_B T}} \quad (3.35)$$

The perturbed Hamiltonian is

$$H' = \frac{Zen_o}{4\pi\epsilon_s r} e^{-q_D r} \quad (3.36)$$

From Fermi Golden rule, the scattering rate is

$$\Gamma(\epsilon_k) = \left[\frac{2\pi e^4 N_i Z^2}{\epsilon_s^2 \hbar^4} \right] N(\epsilon_k) \left[\frac{1}{q_D^2 (q_D^2 + 4k^2)} \right] \quad (3.37)$$

The scattering rate given in equation (3.37) is valid within the Brooks-Herring model so long as q_D in the denominator is large enough so that the scattering rate does not diverge.

3.3.6 Alloy Scattering

In the pure group IV-VI, III-V and II-VI compound semiconductors, the introduction of alloys cause an additional disruption to the periodic potential of crystal. In *TNL-TS* simulator the alloy scattering rate is given as

$$\Gamma(\varepsilon_k) = \frac{3\pi m^*}{8\sqrt{2}\hbar^4} [x(1-x)] [\gamma(\varepsilon_k)]^{3/2} \frac{d\gamma(\varepsilon_k)}{d\varepsilon} \Omega |\Delta V|^2 \quad (3.38)$$

where x is the molar fraction, the volume of the unit cell Ω is given by $a_o^3/4$ where a_o is the lattice constant, and ΔV characterizes the strength of the perturbing potential.

3.3.7 Piezoelectric Scattering

The piezoelectric scattering should dominate deformation potential scattering at low enough temperatures in crystals having the piezoelectric effect. The scattering rate, in the elastic and the equi-partition approximation, is then of the form;

$$\Gamma(k_0) = \frac{m^*k_B T}{4\pi\hbar^3 k\rho} \left(\frac{e e_{pz}}{\epsilon v_s}\right)^2 \ln\left(1 + 4\frac{k^2}{q_D^2}\right) \quad (3.39)$$

Here, the screening factor, q_D , is taken as the Debye wavevector (see equation 3.35) and e_{pz} is the piezoelectric constant of the semiconductor material.

3.3.8 Dislocation Scattering

The abrupt changes in the periodic arrangements of atoms along a line in the lattice are defined as dislocation e.g. the epitaxial growth of GaN over Al₂O₃ substrate has a 13.8% lattice mismatch and a 34% mismatch in the thermal expansion coefficient. Dislocations are typically formed due to the large lattice mismatch of GaN with the substrates on which it is epitaxially grown (Si, SiC and Sapphire). This scattering mechanism becomes the dominant one at doping levels equivalent with the volume concentration of traps introduced by dislocations. The scattering rate can be expressed as

$$\Gamma(\varepsilon_k) = \left[\frac{e^4 N_{dis} m_d}{\varepsilon_s^2 \hbar^3 c^2} \right] \left[\frac{\lambda^4}{\left(1 + \frac{8\lambda^2 m_d (1 + \alpha \varepsilon_k)}{\hbar^2}\right)^{3/2}} \right] \left(1 + \frac{4\lambda^2 m_d \varepsilon_k (1 + \alpha \varepsilon_k)}{\hbar^2}\right) (1 + 2\alpha \varepsilon_k) \quad (3.40)$$

Here c is the velocity of light, N_{dis} is the line dislocation density and λ is the screening factor and is given by

$$\lambda = \sqrt{\frac{\varepsilon k_B T}{e^2 n_s}} \quad (3.41)$$

Where, n_s is the effective screening concentration.

3.3.9 Carrier-Carrier Scattering

Carrier-carrier interactions, apart from degeneracy effects, may be treated as a scattering process within the Monte Carlo algorithm on the same footing as other mechanisms. The two-body coulomb interaction can still be represented by a screened potential. It starts from the realization that a sum over the distribution function associated with each electron is simply an ensemble average of a given quantity. The individual carrier-carrier interaction via a screened Coulomb potential of the form is given by

$$V(r) = \frac{e^2}{\epsilon r} e^{-\beta r} \quad (3.42)$$

Here, β is inverse Debye screening length and the transition probability of two electrons from the wave-vectors k and k_0 to k' and k'_0 is obtained using the *Fermi Golden rule*. Thus, the scattering rate for a electron-electron scattering can be expressed as

$$\Gamma(k_0) = \frac{2m^*e^4}{\hbar^3\epsilon^2V} \sum_k \frac{|k-k_0|}{|k-k_0|^2+\beta^2} \quad (3.43)$$

Here m^* is the electronic effective mass depends upon the position of electron on phase space, e is the electronic charge, V is the screened potential refer to equation (3.42) and ϵ is the dielectric constant of the material.

3.3.10 Impact Ionization Scattering

The impact ionization scattering rate depends on the volume of the available phase space and the average squared transition matrix element $|M_{ii}|^2$ within that phase space. The importance of the impact ionization rate around the threshold energy depends on the high energy tail of the carrier distribution and the ratio of the impact ionization rate to the phonon scattering rates. A carrier, being able to impact ionization, has to survive to energies above the threshold, emitting less phonon than the bulk of the particles. The carrier distribution above the threshold energy therefore strongly depends on the dissipation processes below the threshold energy. If the carrier has survived to impact ionization enabling energies, the occurrence of impact ionization has to be relevant compared to phonon scattering. The impact ionization rates are given by the below equation which also validate the Keldysh formulas in modified form,

$$\Gamma(\varepsilon_k) = \Lambda^{ii}(\varepsilon_k - \varepsilon_{th}) \quad (3.44)$$

Here,

$$\Lambda^{ii} = \frac{2\pi}{\hbar} |M_{ii}|^2 \frac{\Omega^3}{N_{cell}} \quad (3.45)$$

Here, M_{ij} is the transition matrix element, Ω is the volume and N_{cell} is the number of cell in the phase space. For more details user may need to go through the reference [17].

3.4 Material Data Base

Zincblende (ZB) Material parameters used in various scattering mechanisms between three valley i.e. Γ , L and X

Parameters	Si	Ge	GaAs	InP	AlAs	InAs	GaP	GaN(ZB)	3C-SiC
ϵ_{∞}	11.7	16.2	10.92	9.61	12.5	12.3	9.11	5.3	6.52
ϵ_s	11.7	16.2	12.9	12.5	14.6	15.15	11.1	9.7	9.72
M (kg/m³)	2329	5320	5370	4810	3720	5680	4140	6087	3200
v_s (m/s)	5220	5400	5220	5220	4280	5500	5220	5220	10000
$D_{a\Gamma}$ (eV)	1.2	2.5	7.01	5	7	5.8	5	8.3	14
D_{aL} (eV)	1.7	2.5	9.2	5	7	5.8	5	8.3	14
D_{aX} (eV)	1.7	2.5	9	5	7	5.8	5	8.3	14
$\hbar\omega_{L\rightarrow\Gamma}^{\Gamma}$ (eV)	0.063	0.037	0.03536	0.043	0.015	0.03	0.051	0.0873	0.12
$\hbar\omega_{L\rightarrow\Gamma}^L$ (eV)	0.063	0.037	0.03536	0.043	0.015	0.03	0.051	0.0873	0.12
$\hbar\omega_{L\rightarrow\Gamma}^X$ (eV)	0.063	0.037	0.03536	0.043	0.015	0.03	0.051	0.0873	0.12
$D_{\Gamma\rightarrow L}$ (eV m^{-1})	0	2.00E+10	1.80E+10	5.06E+10	7.02E+10	5.59E+10	5.10E+10	1.80E+10	9E10
$D_{\Gamma\rightarrow X}$ (eV m^{-1})	0	1.00E+11	1.00E+11	4.98E+10	7.30E+10	6.35E+10	5.86E+10	1.00E+11	9E10
$D_{L\rightarrow\Gamma}$ (eV m^{-1})	0	2.00E+10	1.80E+10	5.06E+10	7.02E+10	5.59E+10	5.10E+10	1.80E+10	9E10
$D_{L\rightarrow L}$ (eV m^{-1})	2.63E+10	3.00E+10	5.00E+10	5.75E+10	8.02E+10	6.35E+10	5.86E+10	5.00E+10	9E10
$D_{L\rightarrow X}$ (eV m^{-1})	2.34E+10	4.10E+10	1.00E+10	4.68E+10	6.63E+10	5.59E+10	5.10E+10	1.00E+10	9E10
$D_{X\rightarrow\Gamma}$ (eV m^{-1})	0	1.00E+11	1.00E+11	4.98E+10	7.30E+10	6.35E+10	5.86E+10	1.00E+11	9E10
$D_{X\rightarrow L}$ (eV m^{-1})	2.34E+10	4.10E+10	1.00E+10	4.68E+10	6.63E+10	5.59E+10	5.10E+10	1.00E+10	9E10
$D_{X\rightarrow X}$ (eV m^{-1})	2.26E+10	9.00E+10	1.00E+11	2.80E+10	3.57E+10	3.36E+10	2.77E+10	1.00E+11	9E10
$\hbar\omega_{\Gamma\rightarrow L}$ (eV)	0	2.32E-02	0.0278	2.22E-02	2.51E-02	1.75E-02	2.56E-02	0.0278	0.0854
$\hbar\omega_{\Gamma\rightarrow X}$ (eV)	0	2.30E-02	0.0299	2.19E-02	2.51E-02	1.92E-02	2.86E-02	0.0299	0.0854
$\hbar\omega_{L\rightarrow\Gamma}$ (eV)	0	2.32E-02	0.0278	2.22E-02	2.51E-02	1.75E-02	2.56E-02	0.0278	0.0854
$\hbar\omega_{L\rightarrow L}$ (eV)	3.89E-02	2.40E-02	0.029	2.43E-02	2.70E-02	1.92E-02	2.86E-02	0.029	0.0854
$\hbar\omega_{L\rightarrow X}$ (eV)	3.72E-02	2.28E-02	0.0293	2.09E-02	2.32E-02	1.75E-02	2.56E-02	0.0293	0.0854
$\hbar\omega_{X\rightarrow\Gamma}$ (eV)	0	2.30E-02	0.0299	2.19E-02	2.51E-02	1.92E-02	2.86E-02	0.0299	0.0854
$\hbar\omega_{X\rightarrow L}$ (eV)	3.72E-02	2.28E-02	0.0293	2.09E-02	2.32E-02	1.75E-02	2.56E-02	0.0293	0.0854
$\hbar\omega_{X\rightarrow X}$ (eV)	5.09E-02	3.07E-02	0.0299	2.57E-02	2.63E-02	1.93E-02	2.66E-02	0.0299	0.0854
$E_L - E_{\Gamma}$ (eV)	0.88	-0.14	0.29	0.59	0.1	0.73	0.18	1.4	1.4
$E_X - E_{\Gamma}$ (eV)	0.08	0.635	0.48	0.85	0.25	1.02	0.52	1.2	2.24
ee_{pz}	0	0	0	0	0	0	0	0.375	0
Δ_{Alloy}	0	0	0	0	0	0	0	0	0
N_{dis}	0	0	0	0	0	0	0	0	0
N_i	0	0	0	0	0	0	0	0	0
ϵ_{th} (eV)	1.23	1.2	1.42	3.1			7.5E6		

Material parameters used in various scattering mechanisms between three valley i.e. Γ , U and Γ_3

Wurtzite (WZ)

Parameters	GaN	AlN	InN	ZnO	2H-SiC	4H-SiC
ϵ_∞	5.28	4.77	8.4	3.7	6.5	6.5
ϵ_s	9.7	8.5	15.3	8.2	9.7	9.66
M (kg/m ³)	6087	3230	6240	5600	3200	3200
v_s (m/s)	7620	9060	3780	6400	1373	1373
$D_{a\Gamma}$ (eV)	8.3	6.2	2.05	14	15	17.5
D_{aU} (eV)	8.3	6.9	4.76	14	15	17.5
$D_{a\Gamma_3}$ (eV)	8.3	7.2	3.83	14	15	17.5
$\hbar\omega_{LO}^\Gamma$ (eV)	0.090811	0.0992	0.073	0.072	0.12	0.12
$\hbar\omega_{LO}^U$ (eV)	0.090811	0.0992	0.073	0.072	0.12	0.12
$\hbar\omega_{LO}^{\Gamma_3}$ (eV)	0.090811	0.0992	0.073	0.072	0.12	0.12
$D_{\Gamma \rightarrow U}$ (eVm ⁻¹)	1.80E+10	1.00E+11	1.00E+11	1.80E+10	7E10	6E10
$D_{\Gamma \rightarrow \Gamma_3}$ (eVm ⁻¹)	1.00E+11	1.00E+11	1.00E+11	1.00E+11	7E10	6E10
$D_{U \rightarrow \Gamma}$ (eVm ⁻¹)	1.80E+10	1.00E+11	1.00E+11	1.80E+10	7E10	6E10
$D_{U \rightarrow U}$ (eVm ⁻¹)	5.00E+10	1.00E+11	1.00E+11	5.00E+10	7E10	6E10
$D_{U \rightarrow \Gamma_3}$ (eVm ⁻¹)	1.00E+10	1.00E+11	1.00E+11	1.00E+10	7E10	6E10
$D_{\Gamma_3 \rightarrow \Gamma}$ (eVm ⁻¹)	1.00E+11	1.00E+11	1.00E+11	1.00E+11	7E10	6E10
$D_{\Gamma_3 \rightarrow U}$ (eVm ⁻¹)	1.00E+10	1.00E+11	1.00E+11	1.00E+10	7E10	6E10
$D_{\Gamma_3 \rightarrow \Gamma_3}$ (eVm ⁻¹)	1.00E+11	1.00E+11	1.00E+11	1.00E+10	7E10	6E10
$\hbar\omega_{\Gamma \rightarrow U}$ (eV)	0.073	0.0992	0.0278	0.073	0.0854	0.0854
$\hbar\omega_{\Gamma \rightarrow \Gamma_3}$ (eV)	0.073	0.0992	0.0299	0.073	0.0854	0.0854
$\hbar\omega_{U \rightarrow \Gamma}$ (eV)	0.073	0.0992	0.0278	0.073	0.0854	0.0854
$\hbar\omega_{U \rightarrow U}$ (eV)	0.073	0.0992	0.029	0.073	0.0854	0.0854
$\hbar\omega_{U \rightarrow \Gamma_3}$ (eV)	0.073	0.0992	0.0293	0.073	0.0854	0.0854
$\hbar\omega_{\Gamma_3 \rightarrow \Gamma}$ (eV)	0.073	0.0992	0.0299	0.073	0.0854	0.0854
$\hbar\omega_{\Gamma_3 \rightarrow U}$ (eV)	0.073	0.0992	0.0293	0.073	0.0854	0.0854
$\hbar\omega_{\Gamma_3 \rightarrow \Gamma_3}$ (eV)	0.073	0.0992	0.029	0.073	0.0854	0.0854
$E_U - E_\Gamma$ (eV)	1.34	0.7	2.71	2.1	1.5	2.5
$E_{\Gamma_3} - E_\Gamma$ (eV)	2.14	1	1.78	2.9	2.27	0
ee_{pz}	0.375	0.92	0.375	0.375	0	0
Δ_{Alloy}	0	0	0	0	0	0
N_{dis}	0	0	0	0	0	0
N_i	1.00E+13	1.00E+13	0	1.00E+13	0	0
\mathcal{E}_{th}						

Here,

- ϵ_s and ϵ_∞ are the static relative permittivity and high-frequency relative permittivity.
- M is density.
- v_s is saturation velocity.
- D_a is acoustic deformation potential.
- D_{x-y} is intervalley deformation potential from x-valley to y-valley.
- $\hbar\omega$ is the polar optical phonon energy.
- $\hbar\omega_{x-y}$ is the intervalley transition optical phonon energy.
- $E_x - E_y$ is valley separation energy between X and Y valley,
- e_{pz} is piezoelectric coefficient.
- Δ_{Alloy} is alloy disorder factor.
- N_{dis} is line dislocation factor.
- N_i is ionized impurity.

3.5 Free Flight Generation

In the TNL-TS (THz Spectroscopy) simulator, the particle motion is assumed to consist of free flights terminated by instantaneous scattering events, which change the momentum and energy of the particle after scattering event. The first task is to generate free flights of random time duration for each particle. This time duration is governed by total time of Monte-Carlo simulation of 20ps which is divided in time steps $dt = 0.4\text{fs}$ giving $N=50000$ steps as a simulation points. The pulse arrival is delayed by the time instant of $\frac{3}{4}$ th of the time period (T) of the applied THz pulse to suppress the intrinsic noise. Assuming these conditions the simulation initialize with 50000 steps over a period of 20ps. Hence, at least one period of the driving frequency is contained in every simulation wherein $f \geq 0.1\text{THz}$. By default total number of electrons is 20000 which is use to invoke the simulation. However, users have flexibility to increase the number of carriers at appropriate location before initializing the simulation for getting more accurate results.

To simulate single cycle THz pulse interaction with electrons for hot carrier dynamics analysis, the probability density function $P(t)$, is required. The product $P(t)dt$ is defined as the joint probability that a particle arrive at time t without scattering after a previous collision occurring at time $t = 0$, and then suffer a collision in a time interval dt around time t . The probability of scattering in the time interval dt around t may be written as $\Gamma[k(t)]dt$, where $\Gamma[k(t)]$ is the scattering rate of an electron of wave vector k . The scattering rate, $\Gamma[k(t)]$, represents the sum of the contributions from each individual scattering mechanism, which are usually calculated quantum mechanically using time dependent perturbation theory. The implicit dependence of $\Gamma[k(t)]$ on time reflects the change in k due to acceleration by internal and external force fields. For electrons subject to time independent THz fields, eqn. (3.9) may be integrated to give the time evolution of carrier wavevector k between collision events as

$$\mathbf{k}(t) = \mathbf{k}(0) - \frac{eE\Delta t}{\hbar} \quad (3.46)$$

where E is the applied THz field and is given as Eq. (3.8).

The scattering rate, $\Gamma[k(t)]$, the probability that a particle has not suffered a collision after a time t is given by $e^{-\int_0^t \Gamma[k(t')]dt'}$. Thus, the probability of scattering in the time interval dt after a free flight of time t may be written as the joint probability

$$P(t)dt = \Gamma[\mathbf{k}(t)] \exp\left[-\int_0^t \Gamma[\mathbf{k}(t')]dt'\right] dt \quad (3.47)$$

Random flight times may be generated according to the probability density $P(t)$ above using, for example, the pseudo-random number generator which generate uniformly distributed random numbers in the range of $[0,1]$. Using a direct method, random flight times sampled from $P(t)$ may be generated according to

$$r = \int_0^{t_r} P(t)dt \quad (3.48)$$

where r is a uniformly distributed random number and t_r is the desired free flight time. Integrating Eq. (3.48) with $P(t)$ given by Eq. (3.47) above yields

$$r = 1 - \exp\left[-\int_0^{t_r} \Gamma[\mathbf{k}(t')]dt'\right] \quad (3.49)$$

Since, in principle $1-r$ is statistically the same as r , Eq. (3.20) may be simplified to

$$-\ln r = \int_0^{t_r} \Gamma[\mathbf{k}(t')]dt' \quad (3.50)$$

Eq. (3.50) is the fundamental equation used to generate the random free flight time after each scattering event, resulting in a random walk process related to the underlying particle distribution function. If there is no external driving field leading to a change of \mathbf{k} between scattering events the time dependence vanishes, and the integral is trivially evaluated. In the general case where this simplification is not possible, it is expedient to introduce the so called self-scattering method in which we introduce a fictitious scattering mechanism whose scattering rate always adjusts itself in such a way that the total (self-scattering plus real scattering) rate is a constant in time [12].

$$\Gamma = \Gamma[\mathbf{k}(t')] + \Gamma_{self}[\mathbf{k}(t')] \quad (3.51)$$

where $\Gamma_{self}[\mathbf{k}(t')]$ is the self-scattering rate. The self-scattering mechanism itself is defined such that the final state before and after scattering is identical. Hence, it has no effect on the free flight trajectory of a particle when selected as the terminating scattering mechanism, yet results in the simplification of eqn. (3.51) such that the free flight is given by

$$t_r = -\frac{1}{\Gamma} \ln r \quad (3.52)$$

The constant total rate (including self-scattering) Γ , must be chosen at the start of the simulation interval (there may be multiple such intervals throughout an entire simulation) so that it is larger than the maximum scattering encountered during the same time interval. In the simplest case, a single value is chosen at the beginning of the entire simulation (constant gamma method), checking to ensure that the real rate never exceeds this value during the simulation.

3.6 Choice of Scattering Angles

Defining a spherical coordinate system around the initial wavevector \mathbf{k} , the final wavevector \mathbf{k}' is specified by $|\mathbf{k}'|$ (which depends on conservation of energy) as well as the azimuthal and polar angles, φ and θ around \mathbf{k} . Typically, the scattering rate, $\Gamma_j[n, \mathbf{k}; m, \mathbf{k}']$, only depends on the angle θ between \mathbf{k} and \mathbf{k}' . Therefore, φ may be chosen using a uniform random number between 0 and 2π (i.e. $2\pi r$), while θ is chosen according to the angular dependence for scattering arising from $\Gamma_j[n, \mathbf{k}; m, \mathbf{k}']$. If the probability for scattering into a certain angle $P(\theta)d\theta$ is integrable, the random angles satisfying this probability density may be generated from a uniform distribution between 0 and 1 through inversion of eqn. (3.28).

Once the scattering mechanism has been selected, the scattering angles have to be calculated in order to determine the initial direction of the next flight. THz Spectroscopy simulator takes into account the polar angular dependence of the scattering rate of electrons in a prototypical polar semiconductor, due to polar optical phonon scattering. The probability density for scattering into an angle θ , relative to the original trajectory of travel just before scattering, is given by

$$P(\theta)d\theta = \frac{\Gamma_{POP}(\theta)d\theta}{\int_0^\pi \Gamma_{POP}(\theta)d\theta} \sim \frac{\sin(\theta)d\theta}{\left(E + E' - 2\sqrt{EE'} \cos\theta\right)} \quad (3.53)$$

where $\Gamma_{POP}(\theta)$ is the scattering rate into a small angle $d\theta$ around the angle θ , E is the energy of the particle before scattering, and $E' = E \pm \hbar\omega_o$ is the final energy corresponding to the emission (lower sign) or absorption (upper sign) of an optical phonon of energy $\hbar\omega_o$. The integral in the numerator is for normalization.

3.7 Ensemble Monte Carlo Simulation

The basic Monte Carlo algorithm described in the sections 3.4 may be used to track a single particle over many scattering events in order to simulate the steady-state behavior of a system. However, for improved statistics over shorter simulation times, and for transient simulation, the preferred technique is the use of a *synchronous ensemble* of particles, in which the basic Monte Carlo algorithm is repeated for each particle in a ensemble representing the (usually larger) system of interest until the simulation is completed. Since there is rarely an identical correspondence between the number of simulated charges, and the number of actual particles in a system, each particle is really a *super-particle*, representing a finite number of real particles. The corresponding charge of the particle is weighted by this super-particle number. The super-particle number can be extracted through algorithms implemented in THz Spectroscopy simulator. An ensemble Monte Carlo simulation in which a fixed time step, Δt , is introduced over which the motion of all the carriers in the system is synchronized. The algorithms illustrate random, instantaneous, scattering events, which may or may not occur during a given time-step. Basically, each carrier is simulated only up to the end of the time-step, and then the next particle in the ensemble is treated. Over each time step, the motion of each particle in the ensemble is simulated independent of the other particles. Nonlinear effects such as carrier-carrier interactions or the Pauli Exclusion Principle and Aufbau Principle are then updated at each times step, as discussed in more detail below. [14] –[16]

The non-stationary one-particle distribution function and related quantities such as drift velocity, valley or sub-band population, etc., are then taken as averages over the ensemble at fixed time steps throughout the simulation. For example, the drift velocity in the presence of the field is given by the ensemble average of the component of the velocity at the n th time step as

$$\bar{v}_z(n\Delta t) \cong \frac{1}{N} \sum_{j=1}^N v_z^j(n\Delta t), \quad (3.54)$$

where N is the number of simulated particles and j labels the particles in the ensemble. This equation represents an estimator of the true velocity, which has a standard error given by

$$s = \frac{\varsigma}{\sqrt{N}} \quad (3.55)$$

where ς^2 is the variance which may be estimated from

$$\zeta^2 \cong \frac{N}{N-1} \left\{ \frac{1}{N} \sum_{j=1}^N (v_z^j)^2 - \bar{v}_z^2 \right\}. \quad (3.56)$$

Similarly, the distribution functions for electrons and holes may be tabulated by counting the number of electrons in cells of k -space. From Eq. (3.55), we see that the error in estimated average quantities decreases as the square root of the number of particles in the ensemble, which necessitates the simulation of many particles. Typical ensemble sizes for good statistics are in the range of 10^4 – 10^5 particles. Variance reduction techniques to decrease the standard error given by Eq. (3.55) may be applied to enhance statistically rare events such as impact ionization or electron-hole recombination.

In the THz Spectroscopy simulator, complete simulation goes in time-domain scale with the application of frequency dependent field $E = E_0 \cos(2\pi f n \Delta t)$ elaborated in Eq. 3.8.

Under THz frequency applied in the y direction, the velocity of each particle is calculated at each time step, where y -component of velocity at the n^{th} time step is represented by [14]–[16].

$$v_{y,p} = v_{y,p-1} + \frac{eE_0 dt}{m^*} \cos(2\pi f n dt) \quad (3.57)$$

Here, $v_{y,p-1}$ is the y -component of the velocity at the previous time-step. The proposed model has flexibility for application of THz pulses coupling in any direction i.e. x , y , z with the thin films. The drift velocity of the carriers under the transient conditions is estimated by the ensemble average of the velocity component at the p^{th} time step and is given as [16];

$$v_d(t) = \frac{1}{N} \sum_{j=1}^N v_y^j(pdt) \quad (3.58)$$

Here, n is the number of total time steps, dt is the time step, N is the number of simulated particles and j labels the number of particles in the ensemble.

Current density is calculated with carrier drift velocity as;

$$J(t) = [N + N_{ii}\alpha_n(E)L_{eff}]ev_d(t) \quad (3.59)$$

Here, N and N_{ii} are the number of initiated particles for simulation and generated particles due to impact ionization process, e is electronic charge and v_d is carrier drift velocity of the particles, L_{eff} is length of region penetrated by high THz field enabling impact ionization process and α_n is the impact ionization coefficient expressed as a function of peak strength of the THz field.

The time dependent current density is converted in to frequency dependent current density by using Fourier transform method.

$$J(\omega) = \int_{-\infty}^{\infty} J(t)e^{i\omega t} dt \quad (3.60)$$

where $J(\omega)$ and $J(t)$ are the current densities in frequency domain and time domain respectively. Since simulation is distributed in the discrete time steps the integration can be viewed as the summation over a time period (a property of the Fourier Transform). Thus, $J(\omega)$ can be written as,

$$J(\omega) = \sum_{j=1}^T J(t_j) (\cos(\omega t_j) + i \sin(\omega t_j)) \quad (3.61)$$

Through frequency dependent current density can be used for extraction of several other parameters like conductivity and absorption coefficient of the material through which THz pulses have passed.

The frequency dependent complex conductivity is computed through Fourier transformation method and is given as [16],

$$\sigma(\omega) = \frac{\sum J(t)(\cos \omega t \quad \sin \omega t)}{\sum E(t)(\cos \omega t \quad \sin \omega t)} \quad (3.62)$$

The absorption coefficient is dependent on conductivity and computed as,

$$\alpha(\omega) = \frac{4\pi\sigma_R(\omega)}{n_r c} \quad (3.63)$$

Here, $\sigma_R(\omega)$ is real part of conductivity, n_r [12] is the real refractive index and c is the velocity of light.

References

1. T.Kurosava, Proc. Internat. Conf. Phys. Semicond., Kyoto 1966; J. Phys. SOC Japan, Suppl. 21, 424 (1966).
2. A.D. Boardman, W. Fawcett and H. D. Ress, Solid State Commun. 6, 305 (1968).
3. W. Fawcett, A. D. Boardman, and S. SWAIN, J. Phys. Chem. Solids 31, 1963 (1970).
4. A.D. Boardman, W. Fawcett, and J. G. Ruch, phys. stat. sol. (a) 4, 133 (1971).
5. D. K. Ferry, Semiconductor Transport (Taylor & Francis, London, 2000).
6. J. P. McKelvey, Solid State and Semiconductor Physics (Krieger Pub. Co., 1982).
7. D.Vasileska, S.M.Goodnick, G.Klimeck, Computational Electronics- Semiclassical and Quantum Device Modeling and Simulation (CRC Press © 2010 by Taylor and Francis Group, LLC).
8. Hockney, R. W., Eastwood, I. W.: Computer Simulation Using Particles. New York: McGraw-Hill. 1981.
9. C. Jacoboni and P. Lugli, The Monte Carlo Method for Semiconductor Device Simulation (Springer-Verlag, Vienna, Austria, 1989).
10. K. Hess, Monte Carlo Device Simulation: Full Band and Beyond (Kluwer Academic Publishing, Boston, MA, 1991).
11. L. I. Schiff, *Quantum Mechanics*, McGraw-Hill Inc., New York (1955).
12. H. D. Rees, J. Phys. Chem. Solids 30, 643 (1969).
13. M. H. Kalos and P. A. Whitlock, *Monte Carlo Methods*, Wiley, New York (1986).
14. T. L. Cocker, D. Baillie, M. Buruma, L. V. Titova, R. D. Sydora, F. Marsiglio, and F. A. Hegmann, arXiv:1705.10350v1 (2017).
15. I. A. Kaplunov, A. I. Kolesnikov, G. I. Kropotov, and V. E. Rogalin, Optics and Spectroscopy, 2019, Vol. 126, No. 3, pp. 191–194.
16. Ronald Ulbricht, Euan Hendry, Jie Shan, Tony F. Heinz, Mischa Bonn, Reviews of Modern Physics, 83, (2011)
17. R. Redmer, J. R. Madureira, N. Fitzer, S. M. Goodnick, W. Schattke, E. Scholl, Field effect on the impact ionization rate in semiconductors, J. Appl. Phys., 87(2), (2000).